EXPERIMENTAL INVESTIGATION OF THE EFFECTS OF WAVEFORM TIP INJECTION ON THE CHARACTERISTICS OF TIP LEAKAGE VORTEX IN A LPT CASCADE

A THESIS SUBMITTED TO
THE GRADUATE SCHOOL OF NATURAL AND APPLIED SCIENCES
OF
MIDDLE EAST TECHNICAL UNIVERSITY

BY

BAYRAM MERCAN

IN PARTIAL FULFILLMENT OF THE REQUIREMENTS
FOR
THE DEGREE OF MASTER OF SCIENCE
IN
AEROSPACE ENGINEERING

FEBRUARY 2012

Approval of the thesis:

EXPERIMENTAL INVESTIGATION OF THE EFFECTS OF WAVEFORM TIP INJECTION ON THE CHARACTERISTICS OF TIP LEAKAGE VORTEX IN A LPT CASCADE

submitted by **BAYRAM MERCAN**, in partial fulfillment of the requirements for the degree of **Master of Science in Aerospace Engineering Department, Middle East Technical University** by,

Prof. Dr. Canan ÖZGEN _____
Dean, Graduate School of **Natural and Applied Sciences**

Prof. Dr. Ozan TEKİNALP _____
Head of Department, **Aerospace Engineering**

Assist. Prof. Dr. Oğuz UZOL _____
Supervisor, **Aerospace Engineering Dept., METU**

Examining Committee Members:

Prof. Dr. Cevdet ÇELENLİGİL _____
Aerospace Engineering Dept., METU

Assist. Prof. Dr. Oğuz UZOL _____
Aerospace Engineering Dept., METU

Assoc. Prof. Dr. Dilek Funda KURTULUŞ _____
Aerospace Engineering Dept., METU

Assoc. Prof. Dr. Sinan EYİ _____
Aerospace Engineering Dept., METU

Dr. Barış GÜMÜŞEL _____
Turkish Engine Industries, TEI

Date: 06.02.2012

I hereby declare that all information in this document has been obtained and presented in accordance with academic rules and ethical conduct. I also declare that, as required by these rules and conduct, I have fully cited and referenced all material and results that are not original to this work.

Name, Last name : Bayram MERCAN

Signature :

ABSTRACT

EXPERIMENTAL INVESTIGATION OF THE EFFECTS OF WAVEFORM TIP INJECTION ON THE CHARACTERISTICS OF TIP LEAKAGE VORTEX IN A LPT CASCADE

MERCAN, Bayram

M. Sc., Department of Aerospace Engineering

Supervisor: Assoc. Prof. Dr. Oğuz UZOL

February 2012, 68 pages

This study presents the results of an experimental study that investigates the effects of uniform/waveform tip injection along the camberline on the total pressure loss characteristics downstream of a row of Low Pressure Turbine (LPT) blades. The experiments are performed in a low speed cascade facility. This injection technique involves spanwise jets at the tip that are issued from a series of holes along the camber line normal to the freestream flow direction. The injection mass flow rate from each hole is individually controlled using computer driven solenoid valves and therefore the flow injection geometrical pattern at the tip can be adjusted to any desired waveform shape, and can be uniform as well as waveform along the camber. Measurements involve Kiel probe traverses for different injection scenarios 0.5 axial chords downstream of the blades. Results show that, instead of performing uniform mass injection along the camberline, by selecting an appropriate waveform injection pattern one can reduce the total loss levels of the blade, including the tip leakage loss as well as the wake losses.

Keywords: Tip leakage flow, Active flow control, Tip injection, Low pressure turbine cascade

ÖZ

DALGA BİÇİMLİ UÇ ENJEKSİYONUNUN DÜŞÜK BASINÇLI TÜRBİN KASKATINDAKİ UÇ SIZINTI GİRDAPLARI KARAKTERİSTİĞİ ÜZERİNDEKİ ETKİSİNİN DENEYSEL İNCELENMESİ

MERCAN, Bayram
Yüksek Lisans, Havacılık ve Uzay Mühendisliği Bölümü
Tez Yöneticisi: Yrd. Doç. Dr. Oğuz UZOL

Şubat 2012, 68 sayfa

Bu çalışma, düşük basınçlı türbin kaskatı arkasında yapılan deneylerle dalga biçimli uç enjeksiyonunun uç sızıntı girdapları karakteristiği üzerindeki etkisini incelemektedir. Deneyler düşük hızlı kaskat test düzeneğinde yapılmıştır. Bu enjeksiyon metodu, kanadın kamber çizgisi boyunca yerleştirilmiş olan deliklerden çıkan ve giriş hava akışı yönüne dik olan jet akışı içermektedir. Her delikten çıkan enjeksiyon kütle akışı bilgisayar yardımıyla birbirinden bağımsız solenoid valflerle kontrol edilmekte, bu sayede kanat ucunda istenilen dalga boyu profili üretilebilmektedir. Dalga boyu şekli hem sabit hızlı olabilmekte hem de farklı geometrilerde olabilmektedir. Deneyler kaskat kanat sütununun 0.5 exsenel veter boyu arkasında Kiel probunun travers mekanizması ile konumlandırılmasıyla yapılmıştır. Sonuçlar, kamber çizgisi boyunca yapılan sabit hızlı uç enjeksiyonu yerine, uygun dalga profili seçilerek toplam basınç kaybının, uç sızıntısı girdabı sayesinde oluşan kayıpların ve kanat arkası iz bölgesi kayıplarının daha verimli düşürülebileceğini göstermektedir.

Anahtar Kelimeler: Uç sızıntı akışı, Aktif akış kontrolü, uç enjeksiyonu, Düşük basınçlı türbin kaskatı

ACKNOWLEDGEMENTS

I am grateful to my supervisor Asst. Prof. Dr. Oğuz UZOL for his professional support, guidance, friendship and encouragement throughout the completion of this thesis work. I deeply appreciate his patience and many efforts to proofread my thesis and papers over and over again.

I would like to thank TÜBİTAK for funding this study as a research project and also METU Center for Wind Energy for providing experimental setup. I would like to thank my teammate Eda DOĞAN for her help. I would like to thank Gökhan AHMET for his brotherhood, and also Hasan, Seyfullah and Sinan.

At last I would like to thank my family for their endless trust and support

TABLE OF CONTENTS

LIST OF SYMBOLS

b	Blade span [mm]
C_μ	Injection momentum coefficient
C_p	Total pressure loss coefficient
$C_{p,p}$	Pitch averaged total pressure loss coefficient
$C_{p,passage}$	Passage averaged total pressure loss coefficient
C_x	Axial chord [mm]
δ	Wake half-width [mm]
η	Wake length scale
H	High range of a pulse width modulated signal
LV	Leakage vortex
M_{inj}	Injection mass flow rate ratio
Ω	Vorticity [1/s]
ps	Pressure side
P_l	Local measured total pressure [Pa]
$\bar{P}_{l,p}$	Pitch averaged local measured total pressure [Pa]
P_i	Inlet total pressure [Pa]
PV	Passage vortex
ρ	Inlet density [kg/m^3]
ss	Suction side
T	Period of a pulse width modulated signal
U_i	Inlet velocity [m/s]
V_d	Wake half-width velocity [m/s]
V_e	External velocity [m/s]
V_{inj}	Injection velocity [m/s]
V_o	Wake center velocity [m/s]
x_d	Wake center horizontal shift [mm]

CHAPTER 1

INTRODUCTION

Main aim in aerodynamic structures is to gain lift. Generated lift is used for different purposes. In a physical manner, to create lift, the pressure difference between two surfaces must be increased. By the nature of the fluids, particles tend to move from high pressure field to the low pressure field. This movement is called tip vortices in rectangular wings and tip leakage vortex in turbomachinery. These vortices have a negative effect on the performance of aerodynamic devices, also vortices are the resources of noise related problems.

In a rotor part of a turbomachinery system, there must exist a clearance gap because of the motion of the blades with respect to the casing. This gap allows working fluid to move from high pressure to low pressure which is called tip leakage vortices. Tip leakage vortices cause efficiency losses and high heat transfer to blade tips because of mixing. In turbine blades, the flow has a much more turning angle and more deflected than compressors, thus have larger pitchwise pressure gradients. This makes the interaction in turbines more stronger (Yamamoto[1]). Typically, %1 clearance causes an increase in stage losses by 1-3 percent (Booth [2]).

The control of tip leakage vortices is trending topic in last ten years. People try to use passive control mechanisms, such as winglet-like structures and squealer tips. Also active control of leakage vortex is still being studied. Main aim in control mechanisms is to decrease the pressure loss within the vortex core, decrease the interaction between the leakage vortex and other secondary flows. Complex flow structure in the passages makes the control phenomena more difficult.

The research reported in this thesis is a specific control method for tip leakage vortices that are created by Low Pressure Turbine (LPT) blades. Through this chapter physics behind the passage flow and leakage vortices, previous studies on leakage control and objectives of this study will be presented.

1.1 Flow Physics

Flow in turbomachines is highly 3-dimensional and there exists complex flow structures interacting with each other. There are mainly three vortex structures within the passage flow, leakage vortex, passage vortex and horseshoe vortex (Figure 1.1). Inlet boundary layer which is caused by the casing endwall extends the both sides of the blades because of adverse pressure gradient and rolls up creating the horseshoe vortex. When this vortex structure enters the passage of the blades, because of the pressure gradient between the pressure side and the suction side of the blades, horseshoe vortex rolls through the suction side. This new vortex is called passage vortex (labeled as PV in Figure 1.1). It is reported that turbulence levels within the passage vortex core is high [3,4]

Tip leakage vortex (labeled as LV in Figure 1.1) is created by the difference between the pressure side and the suction side of the blade.Flow particles tend to move from pressure side to suction side. For sharp-ended blades, a separation bubble followed by a reattachment zone occurs [5]. Heyes and Hudson [6] showed that there exists a low pressure region near the pressure side of the tip gap confirming the separation bubble.Yaras et al. [7] has done velocity measurements within the gap for different gap heights and examined that velocity does not change significantly, which results that flow is accelerated at the gap inlet. At the gap exit, flow velocity is high and has an oblique angle relative to the passage flow. This interaction between gap flow and passage flow creates the leakage vortex. Leakage vortex causes high momentum fluid mix up with the boundary layer and low momentum fluid with the mainstream resulting a decrease in total efficiency.

Bindon [8] examined the loss created by the tip clearance gaps and the flow in the gaps. It is stated that there is a dramatic loss increase after the midchord of the blades when there is a gap between the blades and the wall. Up to midchord, the loss characteristics are same for the no-gap case and gap-case. Tip gap creates new flow patterns. Also it is noted that the clearance loss is linear with the gap size.

Yamamoto [1] studied the interactions between the tip leakage vortex and passage vortex. A sample flow pattern in a passage is shown in Figure 1.1 presented by Yamamoto [1]. He stated that when the gap is small (%1.3 span) there is no strong interaction between these two vortices. When the gap size increases, the interaction increases because of the increase of size of the leakage vortex, weakening the passage vortex. Also he studied the effect of tip clearance loss with different flow incidence angles and the stated that net loss mechanism created by tip gaps becomes more important near the design point (i.e. zero flow incidence angle).

Heyes and Hudson [6] showed that when size of the tip clearance increases, the turning angle drops which creating the loss mechanism. Also it is shown that there is a low pressure region near the pressure side at the tip caused by a separation bubble at the tip.

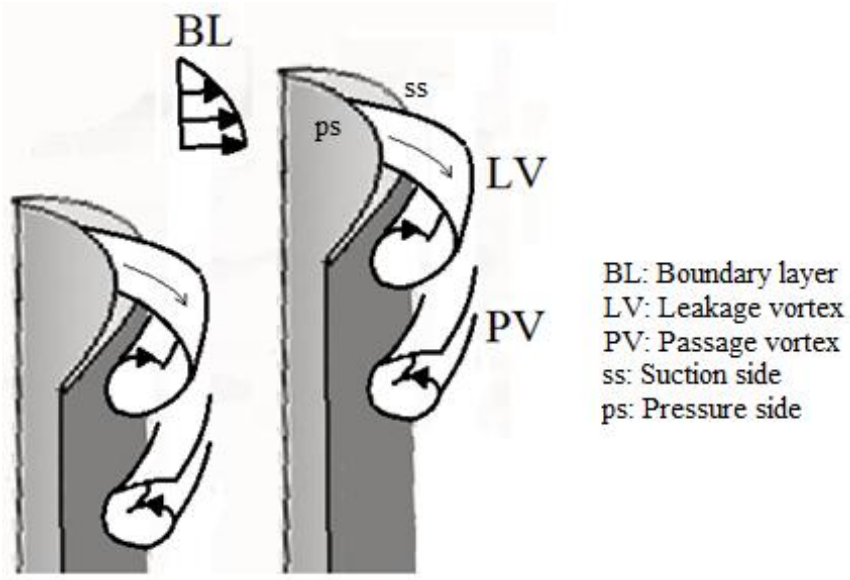

Figure 1.1 Flow patterns in a passage flow

It is known that as the tip clearance gets bigger, loss levels become elevated (Bindon [8]). The physical phenomenon in a tip leakage flow and the basic flow patterns were investigated by Bindon [5] and it's been shown that there is no single flow pattern in tip leakage flows and the leakage mechanism is quite complex, which is also investigated in detail by many other researchers (e.g. Sieverding [9], Gregory-Smith [10], Langston [11]).

1.2 Previous Studies

In past studies several different methods were investigated to control the effects of the tip leakage. These methods generally divide into two groups, i.e. passive and active control. Dey and Camci [12] used tip platform extensions, structures like winglets, to control the tip leakage flow. They conclude that suction side extensions only change the location of the leakage vortex but do not change the pressure loss within the vortex. They also noted that pressure side extensions are highly efficient to reduce the pressure loss, this extension type also reduces the momentum that leaks to the suction side. Van Ness II et.al [13] examined squealer tips as a control mechanism and investigated that the leakage mass flow and size of the tip leakage vortex reduces. Also the size of the casing separation bubble is decreased. Van Ness II et.al [13] also used plasma actuators to control the leakage flow and noted that the strength of the clearance flow is weakened. Rao and Camci [14] injected air through coolant holes at the tip and observed a reduction in total pressure loss within the vortex. The size of the leakage vortex was also reduced.

1.3 Objectives

The objective of this study is to investigate the effects of camberwise modulated waveform tip injection on the characteristics of leakage of a low pressure turbine cascade. This injection technique involves spanwise jets at the tip that are issued from a series of holes along the camber line normal to the freestream flow direction.

The injection mass flow rate from each hole is individually controlled using computer driven solenoid valves and therefore the flow injection geometrical pattern at the tip can be adjusted to any desired waveform shape, and can be uniform as well as waveform along the camber. The experiments are conducted at a blow-down low speed cascade facility and the measurements involve Kiel probe traverses for different injection scenarios 0.5 axial chords downstream of the blades.

The presentation of this thesis is structured on two main parts, the experimental procedure, and results obtained from the measurements

The experimental setup covering the details of the wind tunnel and the cascade blade row is given in Chapter 2.The injection system components, solenoid valves, data acquisition methods and measurement conditions are also presented in this chapter.

Chapter 3 presents the results of the total pressure measurements. The characteristics of mixed flow compressors, the explanation of small turbojet engine design problem and the structure of the optimization problem is mentioned. The final design generated from the results of optimization study is presented in this chapter.

Chapter 4 includes summary and conclusions as well as the future work that can be done in order to improve the study.

CHAPTER 2

EXPERIMENTAL PROCEDURE

2.1 Wind Tunnel and Cascade Blade Row

In this study, the experiments are performed in a continuous-flow blower configuration wind tunnel located in the Aerospace Engineering department in Middle East Technical University which is shown in Figure 2.1. The wind tunnel consists of a radial, double intake blower with a diameter of 0.6 m driven by a frequency controlled 18.5 kW AC electric motor, a 2.6 m long rectangular to square transitional diffuser with a 7 deg diffusion angle, a 1.85 m long 1.1 x 1.1 m^2 square cross-section settling chamber, a 0.915 m long contraction section with an area ratio of 3.36 and followed by a square to rectangular transition duct with an area ratio of 3.36. The transition profiles of the contraction section and the duct are selected as hyperbolic tangent function. Design details of the wind tunnel are presented by Ostovan [15].

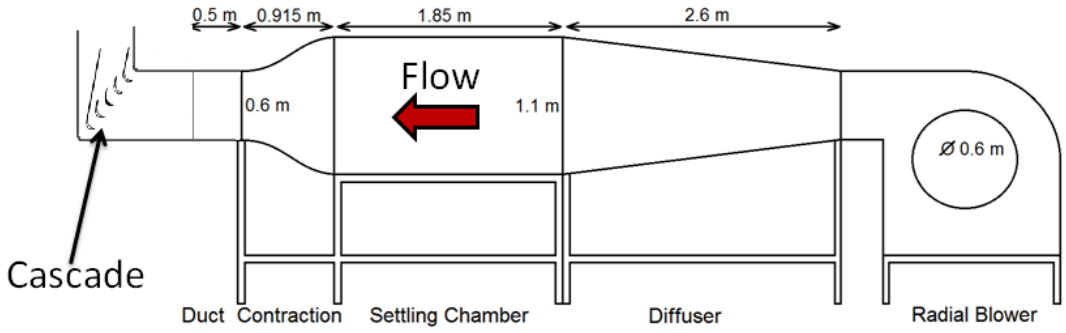

Figure 2.1 Sketch of the Active Flow Control Wind Tunnel

The fully transparent test section which is shown in Figure 2.2 is made out of 0.01 m thick plexiglass and having an inlet area of 0.6 x 0.3 m^2. There consist of single row LPT blades which have a T106 blade profile. There are five blades in the row each having an axial chord of 0.125 m and a total flow turning angle of 100 degrees. Total span of the blades are 0.297 m and the spacing between the blades are 0.128 m. the clearance is about %1 of total span which is accepted as "nominal gap" in the literature. Four of the blades are made out of transparent material (Figure 2.3.a) except for the test blade at the center of the blade row which is painted black (Figure 2.3.b). The blades are positioned with a pitch to chord ratio about 1 and at zero degrees of angle of attack with respect to free stream velocity. Properties of the low-speed wind tunnel and the cascade blade row are given in Table 2.1.

Figure 2.2 Transition duct and transparent test section with the blade row

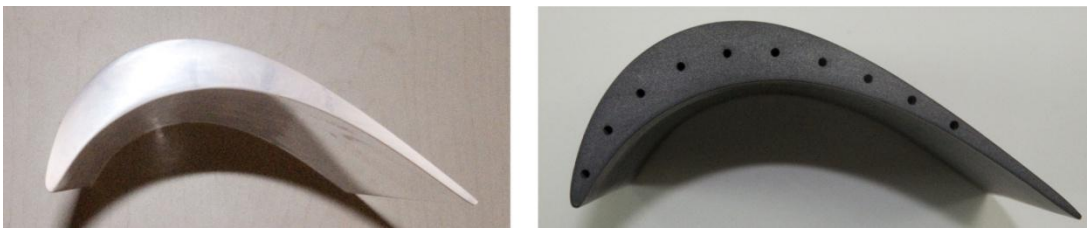

Figure 2.3 Transparent LPT blade (left) and the test blade with the injection holes (right)

Table 2.1 Properties of the low-speed wind tunnel and the cascade row

Wind Tunnel	
Motor Power (kW)	18.5
Blower Diameter (m)	0.6
Diffuser Length (m)	2.6
Diffusion Angle	7
Settling Chamber Length (m)	1.85
Contraction Section Length (m)	1.415
Contraction Area Ratio	3.36
Test Section Inlet Area (m^2)	0.6x0.3
LPT Cascade Test Section	
Airfoil	T-106
Number of Blades	5
Axial Chord (m)	0.125
Span (m)	0.297
Spacing (m)	0.128
Tip Clearance (m)	0.003
Turning Angle	100

2.2 Air Injection System

As discussed before middle blade in the row is marked as “test blade”. There are 10 injection holes distributed through the camberline of the blade each having a diameter of 2.4 mm. Pressurized air for the tip injection system is attained by using an air compressor. The pressurized air is collected in a smaller pressurized tank (Figure 2.4), to which ten solenoid valves are connected. To stabilize the pressure of the air inside the small tank, two pressure regulators are placed between the compressor and the pressurized tank.

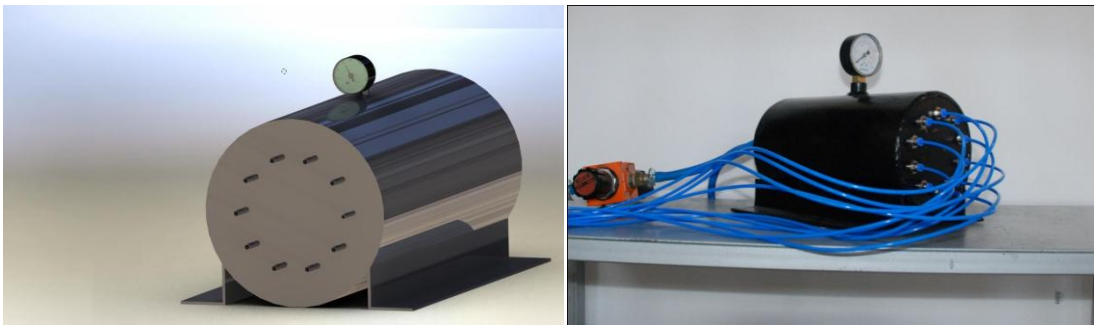

Figure 2.4 Detailed drawing of the pressurized tank (left) and manufactured pressure tank (right) [15]

Between the injection holes and the tank ten solenoid valves are placed. These solenoid valves are computer controlled separately so that different amounts of mass flow could be injected from each hole allowing us to generate different injection waveform patterns. Solenoid valves are controlled by creating pulsed width modulated (PWM) signals by using two different National Instruments signal output cards. Strength of PWM signal is only controlled by a single parameter called duty cycle (Figure 2.5). by changing the duty cycle, the voltage which supplies the solenoid valves is controlled. Supply voltage directly affects the aperture ratio of the valves, in other words, the injection mass flow rate.

As seen in Figure 2.5, PWM signal consists of two parts. First one is called the high range where the supplied voltage is transferred to the control mechanism. Second part is called low range and the control mechanism is not supplied. Whole period of the signal is marked as T, and the high range is marked as H. Ratio of these two values determines the duty cycle of the PWM signal. When duty cycle is equal to %1, valves are totally closed so that no mass is injected. When duty cycle reaches %99, the valves are fully open.

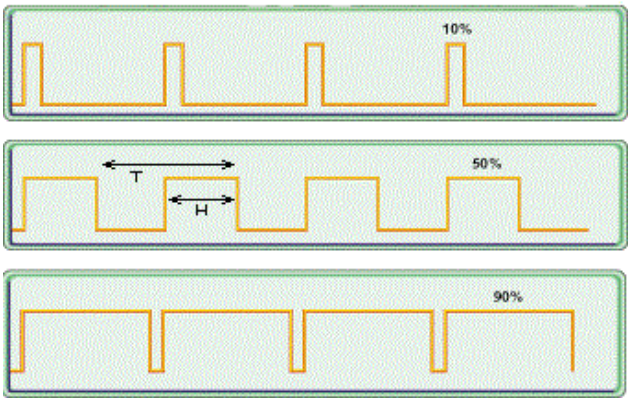

Figure 2.5 Example for a Pulse Width Modulated (PWM) signal

In first sight, it can be thought that there is a linear dependence between duty cycle and aperture ratio of the valves, but it is not so. For each valve this relation changes. To avoid instability problems in the injection system, this relation is measured for each valve. An example of the relation between duty cycle and aperture ratio is presented in Figure 2.6.

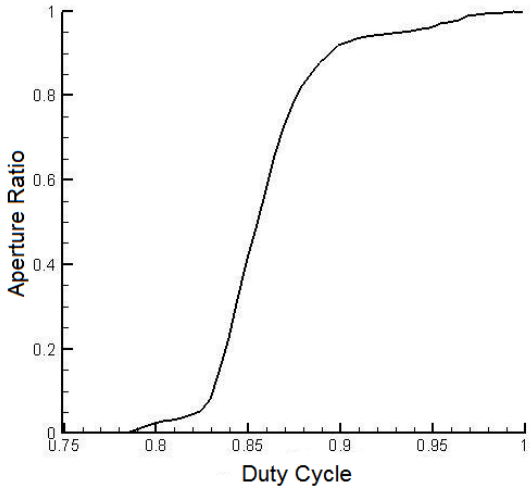

Figure 2.6 Relation between the duty cycle of PWM signal and the aperture ratio of the solenoid valves

To detect the stability of the injected air, injection velocity measurements are conducted by using a single sensor constant temperature anemometry at the exit of each hole at a desired velocity of 85 m/s [15]. Within a 15 minute time interval, mean injection velocity of ten holes are measured as 84.8 m/s, and maximum

standard deviation is 0.669 m/s. Mean velocities and the error bars of the injection holes can be seen in Figure 2.7.

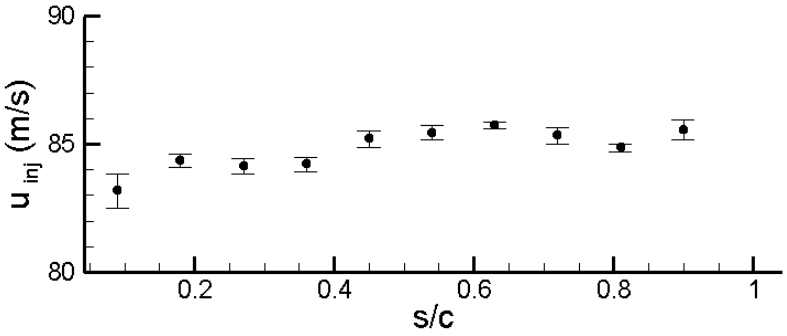

Figure 2.7 Stability measurements in front of each injection holes

2.3 Total Pressure Measurements, Traverse System and Data Acquisition

Through this work all pressure measurements are acquired using Scanivalve DSA-3217 multichannel pressure module. The pressure module has 16 independent channels, half of which it have a range of 0.5 psi and half of it have a range of 1 psi. all the measurements are conducted with a sampling rate of 200 Hz and a sampling time of 2 seconds.

To get data on the desired plane on the wake of the blade row, tri-axial Velmex traverse mechanism is used. The traverse mechanism has a resolution of 0.00635 mm. control of the traverse mechanism is integrated to the LabView program.

2.4 Time-Resolved Particle Image Velocimetry Setup

Time-resolved Particle Image Velocimetry (Tr-PIV) system consists of a 30 mJ/pulse Nd:YLF high-speed laser and a 12-bit high-speed camera that has the capability to operate at 1.5 kHz at a 4 megapixel resolution. A 105mm Sigma Macro lens is used with an aperture setting of f#4. Glycol mixed with water (i.e. commercial fog fluid) is used for seeding the flow. On each measurement plane and for each injection

scenario, 200 image pairs are acquiredand averaged with respect to time, i.e. steady. While processing the images, 64x64 pixels interrogation areas are used with an overlap of 50%. During the post-processing a Gaussian global validation test and a local median test are used to validate the vector maps. Tr-PIV experimental setup and the cascade test section setup can be seen in Figure 2.8.

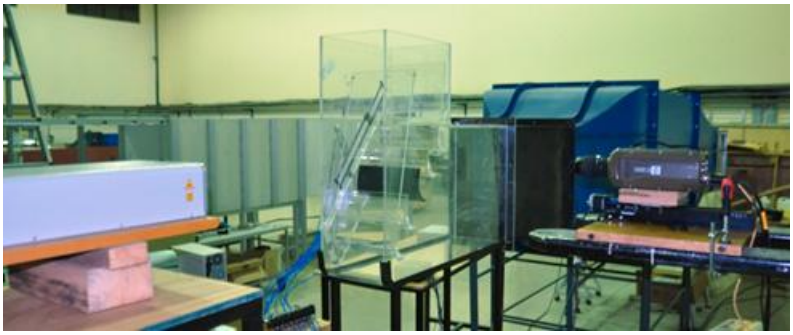

Figure 2.8 Time-resolved Particle Image Velocimetry (Tr-PIV) measurement setup

2.5 Measurement Conditions

Through this work, total pressure measurements are taken by traversing a Kiel probe with a shield diameter of 3.175 mm on a plane which is located 0.5 axial chords downstream of the blade row as shown in Figure 2.9 with a blue line. Total survey area is 25 x 5 cm^2 covering a spanwise region of %84 to %100 span and about two blade passages in pitchwise direction. The spatial resolution of the traversed grid is 2.5 mm. Tr-PIV measurements are conducted in four different spanwise locations, 0.5b, 0.75b,0.85b, 0.95b as shown in Figure 2.10. Total survey area is 34.5 x 27.5 cm^2 covering wake of the test blade and the wake of the neighboring blade. Spatial resolution of the measured data is approximately 6 mm.

All measurement data are taken for a free stream velocity of 10 m/s, which corresponds to a Reynolds number of 86000 based on the axial chord of the blades and the inlet velocity.

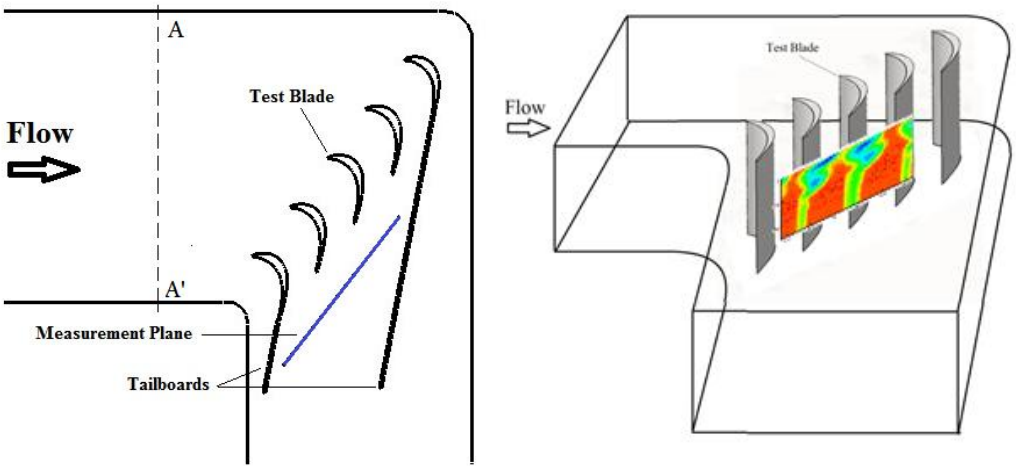

Figure 2.9 Sketch of the total pressure measurement plane, upper view (left), 3-d view (right)

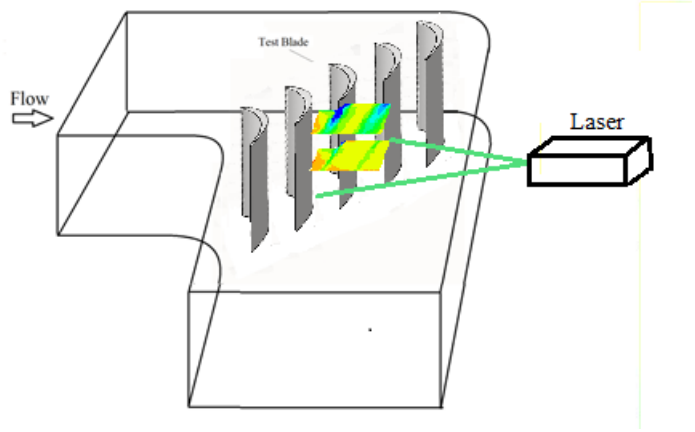

Figure 2.10 Sketch of the Tr-PIV measurement plane

2.6 Injection Scenarios

To investigate the effects of tip injection on tip leakage characteristics two different perspectives are used. First, the effect of injection mass flow rate is investigated. The tip injection is usually characterized by the injection mass flow rate ratio, M_{inj} (Rao and Camci [14]), which is defined as the ratio of the injection mass flow rate to the total inlet mass flow rate. Definition of injection mass flow rate is given in Equation 2.1.

$$M_{inj} = \frac{Sumoft\ heinjectedmassflowin \quad 10\ holes}{Totalinletmassflow} \qquad \text{Equation 2.1}$$

Characteristics of tip injection also depend on injection momentum coefficient, C_μ, as defined in Equation 2.2. Note that although the M_{inj} values may be the same for different waveform patterns, injection momentum coefficients may be different which is defined by Equation 2.2.

$$C_\mu = \frac{M_{inj}\, V_{inj}}{q_i b C_x} \qquad \text{Equation 2.2}$$

To investigate the effects of injection mass flow rate, three different injection scenarios with uniform pattern (i.e. injection velocity is constant for all 10 holes) with different injection velocities are selected.

To investigate the effects of injection waveform pattern, injection mass flow rate is kept constant while changing the waveform pattern. For M_{inj}=0.01, reversed triangular, triangular and corresponding uniform waveform patterns are selected. For M_{inj}=0.0125, sinusoidal, reversed sinusoidal and corresponding uniform waveform patterns are selected. For triangular and sinusoidal waveforms, injection velocity is 0 m/s at the injection hole which is located near the leading edge while injection velocity is 80 m/s at the hole located near the trailing edge. For the reversed triangular and reversed sinusoidal waveform patterns, injection velocity is 0 m/s at the injection hole which is located near the trailing edge while 80 m/s at the hole located near the leading edge. A schematic description of the injection scenarios are given in Figure 2.11 and detailed injection parameters are given in Table 2.2.

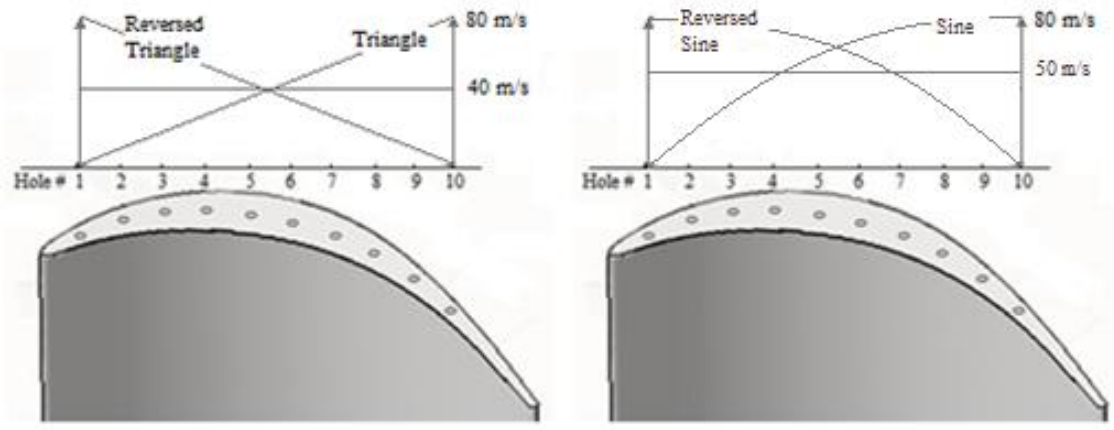

Figure 2.11 Injection waveforms for M_{inj}=0.01 (left) and M_{inj}=0.0125 (right)

Table 2.2 Injection scenario parameters

M_{inj}	Waveform Pattern	C_μ	V_{inj}, Hole #1	V_{inj}, Hole #10
0.001	Triangular	0.054878585	0	80
0.001	Reversed Triangular	0.054878585	80	0
0.001	Uniform	0.038992679	40	40
0.00125	Half-Sine	0.077983309	0	80
0.00125	Reversed Half-Sine	0.077983309	80	0
0.00125	Uniform	0.060926061	50	50
0.002	Uniform	0.155970715	80	80

2.7 Measurement and Working Point Uncertainties

The uncertainty in total pressure measurements is estimated to be less than 7% as also reported in Uzol and Camci [16]. The variations in the inlet velocity and the injection velocity levels are less than 1% and 0.7%, respectively, during the experiments (Mercanet al. [17]).The spatial displacement accuracy of the PIV cross-correlation algorithm is less than approximately 0.1 pixel, which is expected to generate a spatial displacement error on the order of less than 1% for a particle displacement of about 5 to 10 pixels (von Ellenrieder and Pothos [18]), which are typically observed in our current measurements. The error due to temporal variations in the laser pulse synchronization is counted as negligible. As to the statistical error

due to using 200 vector maps for averaging, Uzol et al. [19] quantified the convergence errors due to using 100 vector maps compared to using 1000 vector maps in a turbulent rotor wake of an axial turbomachine. Maximum observed errors in mean velocities and the turbulent kinetic energy was around 5% and 8%, respectively. Therefore in this study statistical convergence errors are expected to be less than those levels.

CHAPTER 3

RESULTS

3.1 Data Analysis Methodology

3.1.1 Total Pressure Analysis

For a better understanding of tip injection on the characteristics of tip leakage flow, a parameter called total pressure loss coefficient is defined (Equation 3.1).

$$C_p = \frac{P_l - P_i}{0.5\rho U_i^2} \qquad \text{Equation 3.1}$$

Here, P_l is the local total pressure, which is measured, P_i is the inlet total pressure. U_i is the inlet velocity. Also another loss parameter called pitch averaged total pressure loss coefficient is defined as in Equation 3.2.

$$C_{p,p} = \frac{\bar{P}_{l,p} - P_i}{0.5\rho U_i^2} \qquad \text{Equation 3.2}$$

In this loss coefficient, $\bar{P}_{l,p}$ is called as the pitch averaged total pressure. To calculate this parameter all total pressure values through the passage (in other words in a pitchwise direction) are averaged.

Pitch averaged total pressure loss coefficients are also used to calculate passage averaged total pressure loss coefficients.

3.1.2 Wake Analysis

For a better understanding of the effects of tip injection, velocity scaling and similarity parameters can be used. Corresponding velocity and length scales are velocity defect within the wake and wake half-width [20, 21]. In nature some wakes are symmetric (i.e. wake of a cylinder, wake of a symmetric airfoil with zero angle of attack). But in turbomachinery flows, wake of a turbine blade is asymmetric. Symmetric and asymmetric wakes can be scaled in a same manner with minor differences. First let us define the basic flow parameters of the wake.

To use the velocity and length scaling first the coordinate system must be rotated in such that the origin of the new coordinate system corresponds to the trailing edge of the turbine blade. As shown in Figure 3.1, y' axis must be parallel to the camberline of the blade, x' axis must be perpendicular to the camberline of the blade. Because the wake is asymmetric, the location of maximum velocity deficit shifts from the vertical axis by an amount of x_d. Minimum velocity within the wake (i.e. wake center velocity) is labeled as V_o, and the external velocity (where the wake is not dominant) is labeled as V_e. Wake half-width, δ, is where the local velocity, V_d, is equal to $0.5(V_e+V_o)$.

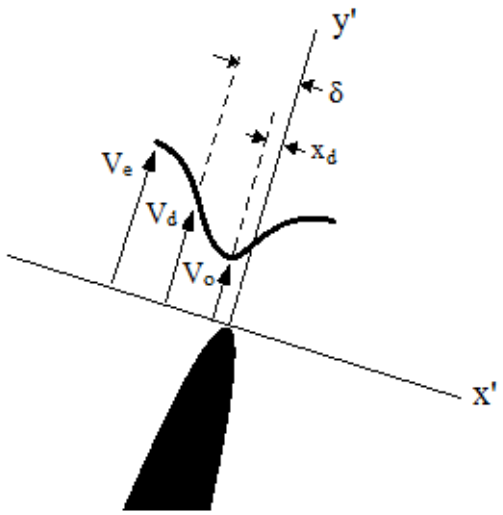

Figure 3.1 Wake scaling schematic and nomenclature

For symmetric wakes, lengths are scaled with δ and velocity is scaled by Equation 3.3.

$$\frac{V_e - V}{V_e - V_o} = \exp(-0.637(x/\delta)^2 - 0.056(x/\delta)^4) \quad \text{Equation 3.3}$$

As seen when proper scaling parameters are used all wake structures become a function of (x/δ). For an asymmetric wake, a simple change is used in scaling because the wake is shifted. Two different wake half-widths are defined for the suction side and the pressure side. These two wake half-widths are used while scaling length parameters. New length scale is given by Equation 3.4

$$\eta = \frac{x - x_d}{\delta_i} \quad \text{where i=ps, ss} \qquad \text{Equation 3.4}$$

For Time-Resolved Particle Image Velocimetry (Tr-PIV) results, velocity and length scaling analysis is done such that effects of tip injection on size of the wake, maximum velocity deficit within the wake, etc. can be investigated. Remember that Tr-PIV measurements are conducted at four different spanwise directions (Figure 2.10). For each spanwise location, velocity and length scaling analysis is used for 12 different streamwise locations as shown in Figure 3.2. In Figure 3.3 scaled wake fields for different spanwise location shown in Figure 3.2 for a plane located at 0.5b with no injection is shown. As seen, all wake structures are one on the top of the other, creating a single curve. By using wake scaling, growth of the wake and damping of the wake can be investigated.

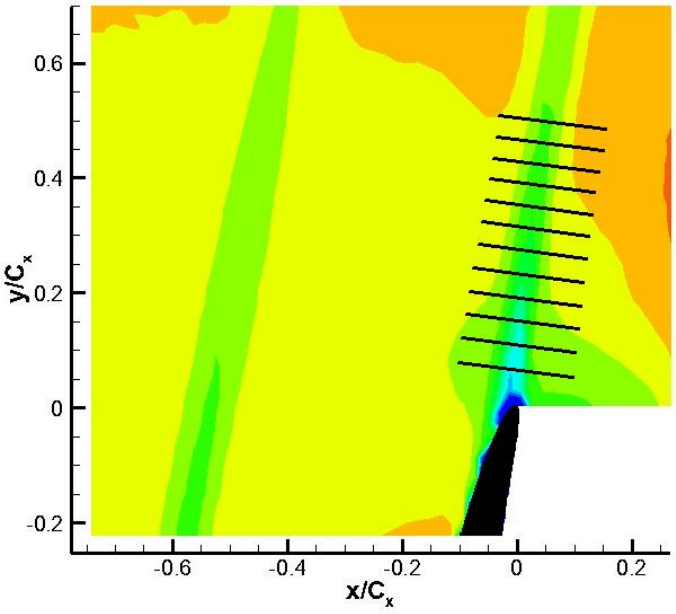

Figure 3.2 Selected spanwise locations for vector and length scaling

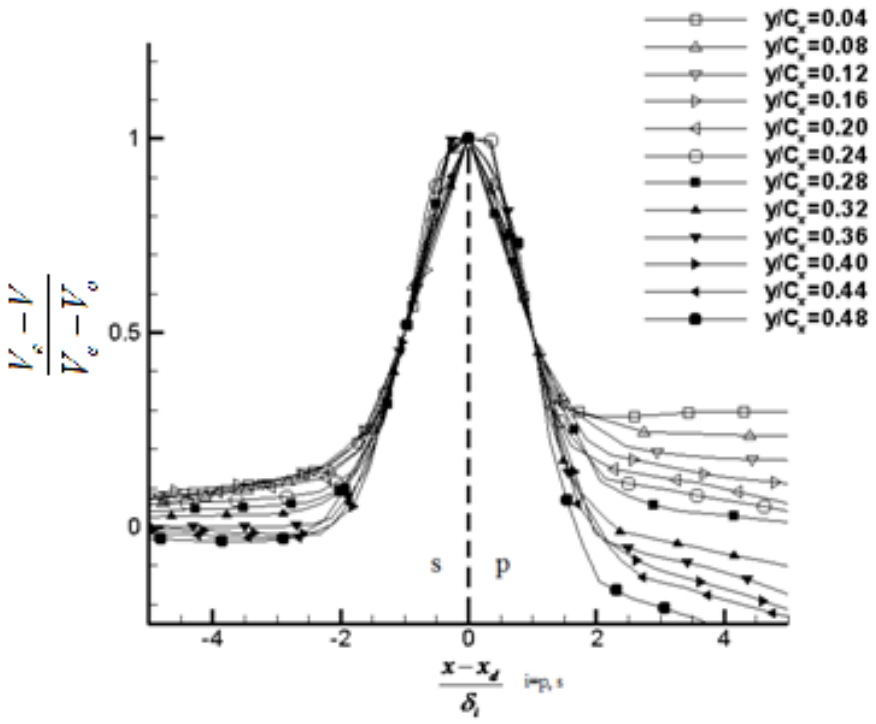

Figure 3.3 Scaled wake field at 0.5b without injection

3.2 Periodicity and Baseline Results

The turning angle of the test section is 90 degrees while the design turning angle of T-106 blades is 100 degrees. To get the periodicity at the downstream of the cascade blade row, tailboards are placed. Figure 3.4 shows the total pressure measurements 0.5 axial chord downstream of the cascade row with and without the tailboards. Without tailboards, distance between two wakes is approximately 14 cm which is about 1.12 times of the spacing of the blades. With tailboards, the distance is 12 cm which is about 0.96 of the spacing of the cascade blades. Also tailboards decrease the pressure loss within the passage.

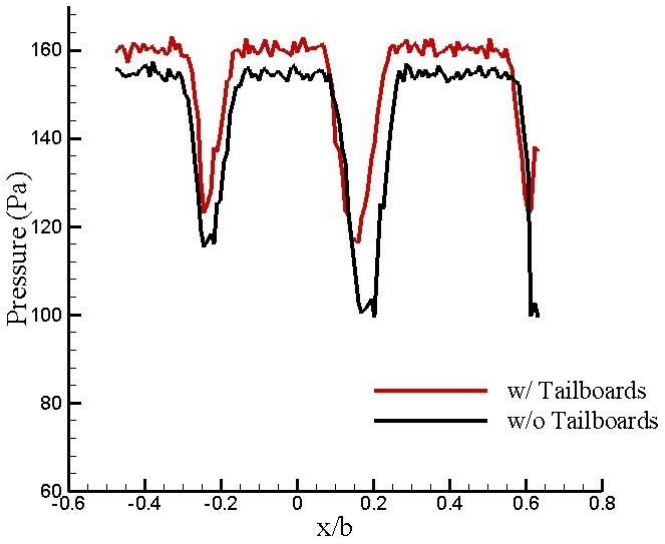

Figure 3.4 Total pressure measurements at 0.5 axial chord downstream with and without the tailboards

For a baseline case, to understand the physical phenomena of the passage flow, a wider survey area is used. Total survey area is 33 x 15 cm^2 covering a spanwise region of %50 to %100 span and about two blade passages in pitchwise direction. Result of the total pressure measurements for the baseline case is shown in Figure 3.5. For all the graphs presented in this work, b is the blade span and the x=0 coordinate is the projection of the trailing edge of the test blade on the measurement plane in downstream location.

First result that can be seen from Figure 3.5 is that flow seems to be periodic. But wake of the test blade is thicker than the neighboring blades. This result is caused by the material which the test blade is manufactured. Above %90 span, there is a pressure loss region for each blade which is labeled as "LV". This flow regime is the tip leakage vortex regime. As explained in the introduction chapter, tip leakage vortex moves through the suction side of the blades. Between %90 and % 80 span there is another low pressure region for each blade which is labeled as "PV". This low pressure regime is caused by passage vortices. There is an interaction between these two vortices (refer to Chapter 1).

Passage region of the test blade is shown with dashed lines in Figure 3.5. The passage region starts from the pressure side of the test blade and goes up to the pressure side of the neighboring blade. This passage region boundaries are used to calculate the pitchand passage averaged total pressure loss coefficient which is defined as in Equation 3.2.

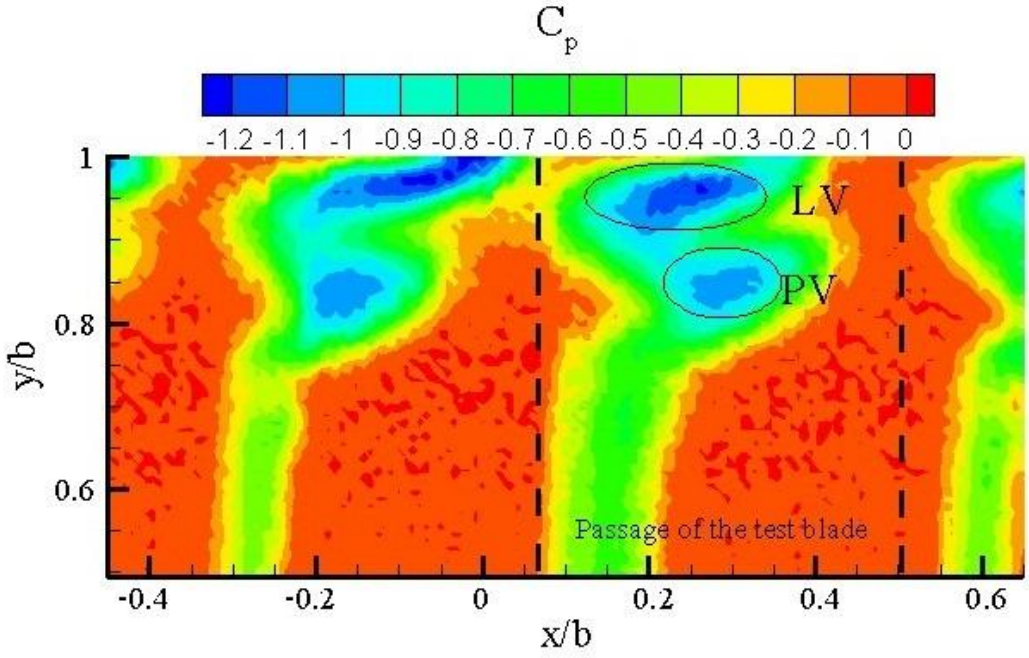

Figure 3.5 Measured total pressure loss coefficient contours 0.5 axial chords downstream of the blade row for no injection case. b=0.3 m is the blade span, x=0 coordinate is the projection of the trailing edge of the test blade on the measurement plane

x=0 coordinate is the projection of the trailing edge of the test blade on the measurement plane. As seen, wake of the test blade does not match up with this coordinating. Tip gap in turbomachines cause a reduction in turning angle. This mismatch is caused by this reduction. Desired turning angle of the flow for T-106 low pressure turbine blades is 99.9 degrees. But in our cascade facility, the flow turning angle is about 96 degrees.

3.3 Effect of Injection Mass Flow Rate

First aim was to understand the effect of injection mass flow rate ratio on the characteristics of the tip leakage flow. For this three different ratios are selected with all having an injection pattern of uniform waveform. Figure 3.6 shows the total pressure loss coefficient contours.

Uniform injection significantly affects the wake characteristics of the blades. Above %90 span, where tip leakage vortex is dominant, tip injection moves the vortex through the endwall. Also the size of the vortex seems to get smaller and within the vortex core pressure loss is decreased with tip injection. But it must be noted that when injection mass flow rate ratio increases, pressure loss within the leakage vortex does not decrease. Leakage vortex of the neighboring blade is also affected by tip injection. Again the size of the vortex and pressure loss within the vortex is decreased. But the relation between injection mass flow rate ratio and the pressure loss within the vortex core is not the same as in the test blade. When the mass flow rate ratio increases, pressure loss levels decrease within the leakage vortex of the neighboring blade.

Passage vortex also seems to be affected by the tip injection (for the regions below %90 span). Injection seems to decrease the interaction between the passage vortex and leakage vortex. For M_{inj}=0.001 and M_{inj}=0.00125 pressure loss within the passage vortex gets increased. By only looking to these two contours, an investigator would say, injection affects the passage vortex in a negative manner, increasing the pressure loss.

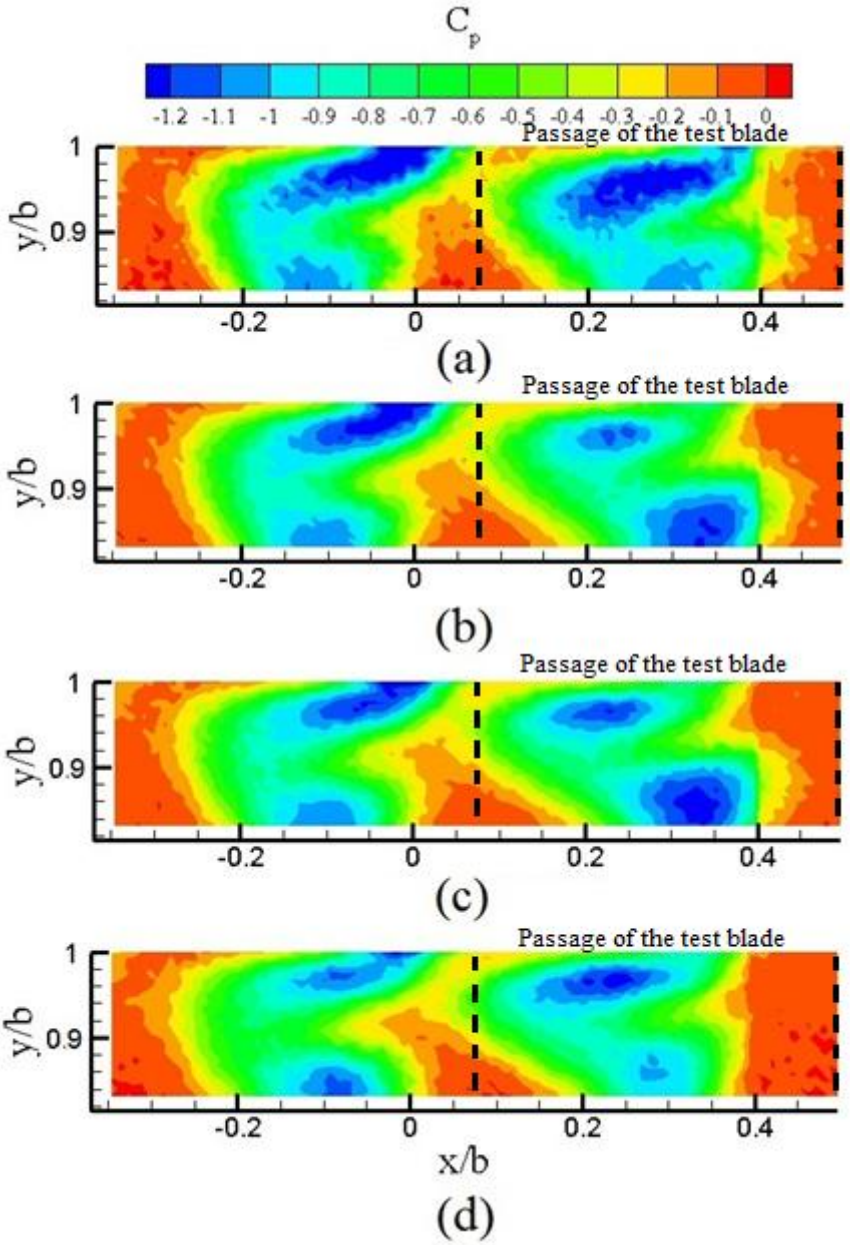

Figure 3.6 Measured total pressure loss coefficient contours 0.5 axial chords downstream of the blade row for four different mass injection ratios using uniform injection from the tip. *b=0.3 m* is the blade span. *x=0* coordinate is the projection of the trailing edge of the test blade on the measurement plane. (a) M_{inj} = 0.0 (b) M_{inj} = 0.001 (c) M_{inj} = 0.00125 (d) M_{inj} = 0.002

But when the total pressure loss coefficient contours for M_{inj}=0.002 is investigated (Figure 3.6.d), it can be easily seen that pressure loss levels in the passage vortex regime is decreased compared to the baseline case. Tip injection does not have a significant effect on the passage vortex of the neighboring blade.

Figures 3.7.a and b show the pitchwise variations of the total pressure loss coefficients at y/b=0.95 (i.e. 95% span) and y/b=0.85 (i.e. 85% span), respectively. These line distributions are extracted from the contour plots presented in Figure 3.6. In all distributions the dip on the right corresponds to the flow downstream of the test blade and the one on the left corresponds to the no-injection blade, which is adjacent to the test blade.

At 95% span, which is within the leakage dominated zone, the mass injection significantly reduces the total pressure loss levels created by the test blade. For M_{inj}=0.001, the wake-like region shrinks in pitchwise direction and the minimum total pressure levels are higher about 30%. Increasing the injection amount on the other hand does not further reduce the total pressure loss, instead a slight pitchwise enlargement of the wake-like region is observed. As to the no-injection blade, it also gets affected from the injection performed on the test blade, however the effects do not seem as significant until M_{inj} reaches a level of 0.002 where some reduction in the total pressure levels is also observed.

At 85% span (Figure 3.7.b), which is mainly out of the leakage zone but more within the wakes of the blades, the wake of the no-injection blade does not seem to get affected at all from the injection performed on the test blade. The wake of the test blade on the other hand gets deeper as the injection is performed both for M_{inj} = 0.001 and 0.00125 and a slight shift to the right in pitchwise direction is also observed. As the M_{inj} value gets higher, at 0.002, the wake deficit gets reduced again, similar to the region closer to the tip. This trend change as the mass injection gets increased could be due to a stronger alleviation of the tip leakage at these high injection mass flow rate values, but more data

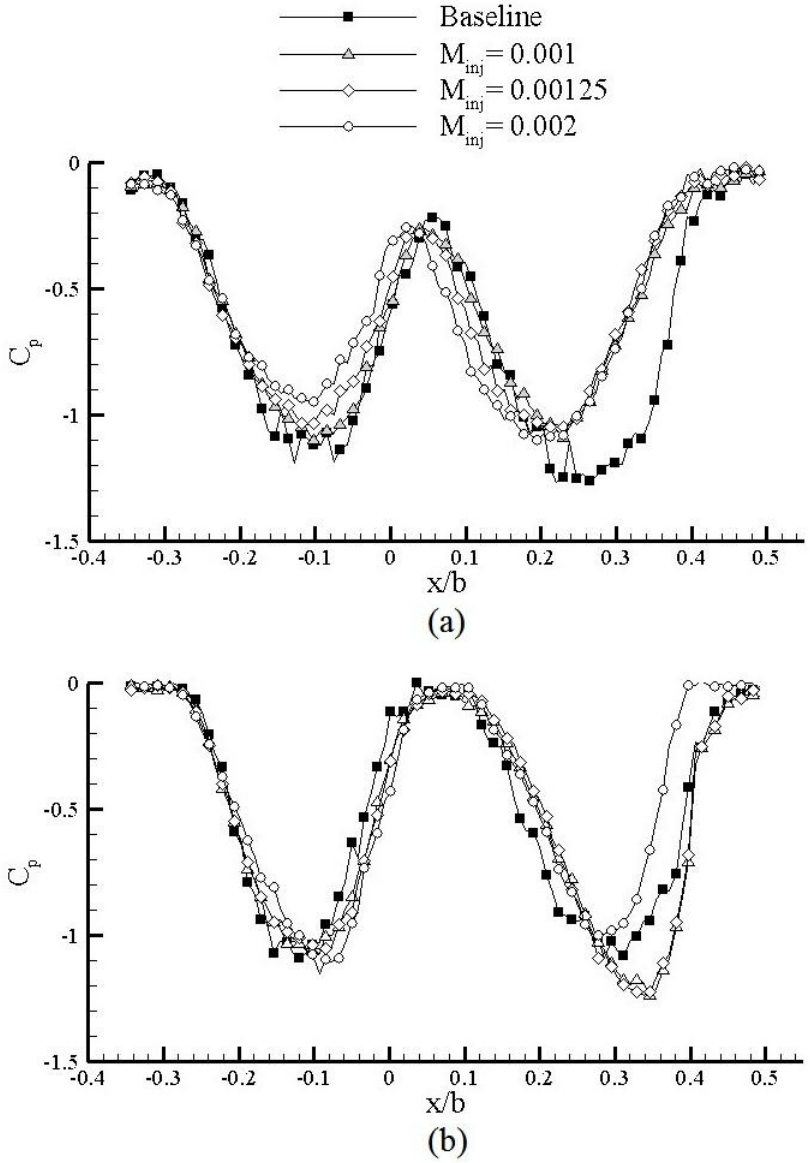

Figure 3.7 Pitchwise total pressure loss coefficient variations at (a) y/b=0.95 and (b) y/b=0.85, 0.5 axial chords downstream of the blade row for four different mass injection ratios using uniform injection from the tip

are needed to further understand this point. These results are also presented byMercan et al. [22].

Figure 3.8 shows the pitch averaged total pressure loss coefficients which are computed using Equation 3.2. It can be seen that for all injection mass flow ratios total pressure loss within the leakage vortex is reduced. For the passage vortex region, most efficient case seems to be uniform injection with M_{inj}=0.002. Other two scenarios does not have a pressure gain within the passage vortex region.

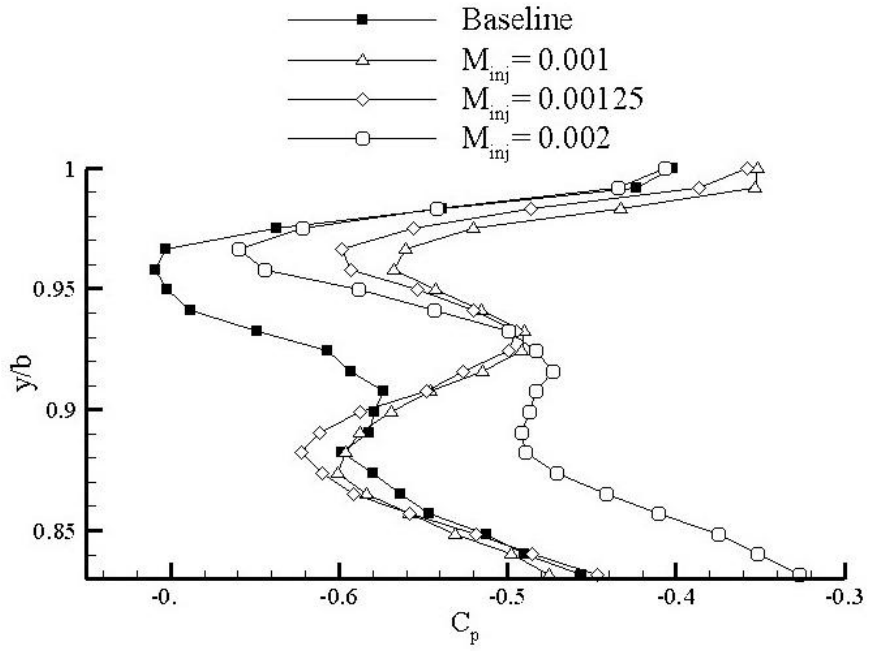

Figure 3.8 Pitch averaged total pressure loss coefficient variations 0.5 axial chord downstream of the blade row for four different mass injection ratios using uniform injection at the tip

Table 3.1 presents the passage averaged total pressure loss coefficients using pitch averaged total pressure loss coefficients and passage boundaries shown in Figure 3.6. Passage averaged total pressure loss coefficients combine the pressure loss levels within the passage vortex zone and leakage vortex zone. As seen, tip injection decreases the

Table 3.1 Passage averaged total pressure loss coefficients and pressure loss reduction levels for different injection mass flow rates

M_{inj}	Waveform Pattern	C_{μ}	$C_{p,passage}$	Pressure Loss Reduction (%)
0	Baseline	0	-0.578	0
0.001	Uniform	0.039	-0.518	10.281
0.00125	Uniform	0.061	-0.531	8.091
0.002	Uniform	0.156	-0.487	15.760

pressure loss levels within a turbine passage. When M_{inj}=0.002, 15% pressure loss reduction is achieved compared to no injection case.

Figure 3.9 shows the inplane velocity magnitude measured by Tr-PIV system for different injection mass flow rates at four different spanwise locations. In these figures, lower right corner is blocked by the test blade and the black zone is the triling edge of the test blade. The flow is from bottom to top.

The wake of the test blade and no-injection blade can be clearly seen at 50% spanwise location and it must be noted that the flow is periodic. First observation from the results is that tip injection has a minimal effect at 50% spanwise location as expected. At 75% span, still tip injection has a minimal effect but when M_{inj}=0.002 there is a slight increase in the velocity deficit within the wake. At 85% span location, where the passage vortices are dominant, injection has an effect on the wake characteristics. When M_{inj}=0.001 and M_{inj}=0.002, velocity deficit within the wake decreases while when M_{inj}=0.00125, there is an increase in the velocity deficit. At 95% span location, for all injection mass flow rates, tip injection has a positive effect, but the most efficient injection case seems to be uniform injection with M_{inj}=0.001 and M_{inj}=0.00125. Also it must be noted that wake of the neighboring blade is effected by the tip injection, velocity deficit within the neighboring blade seems to be decreased. These results can be supported by mean vorticity contours shown in Figure 3.10.

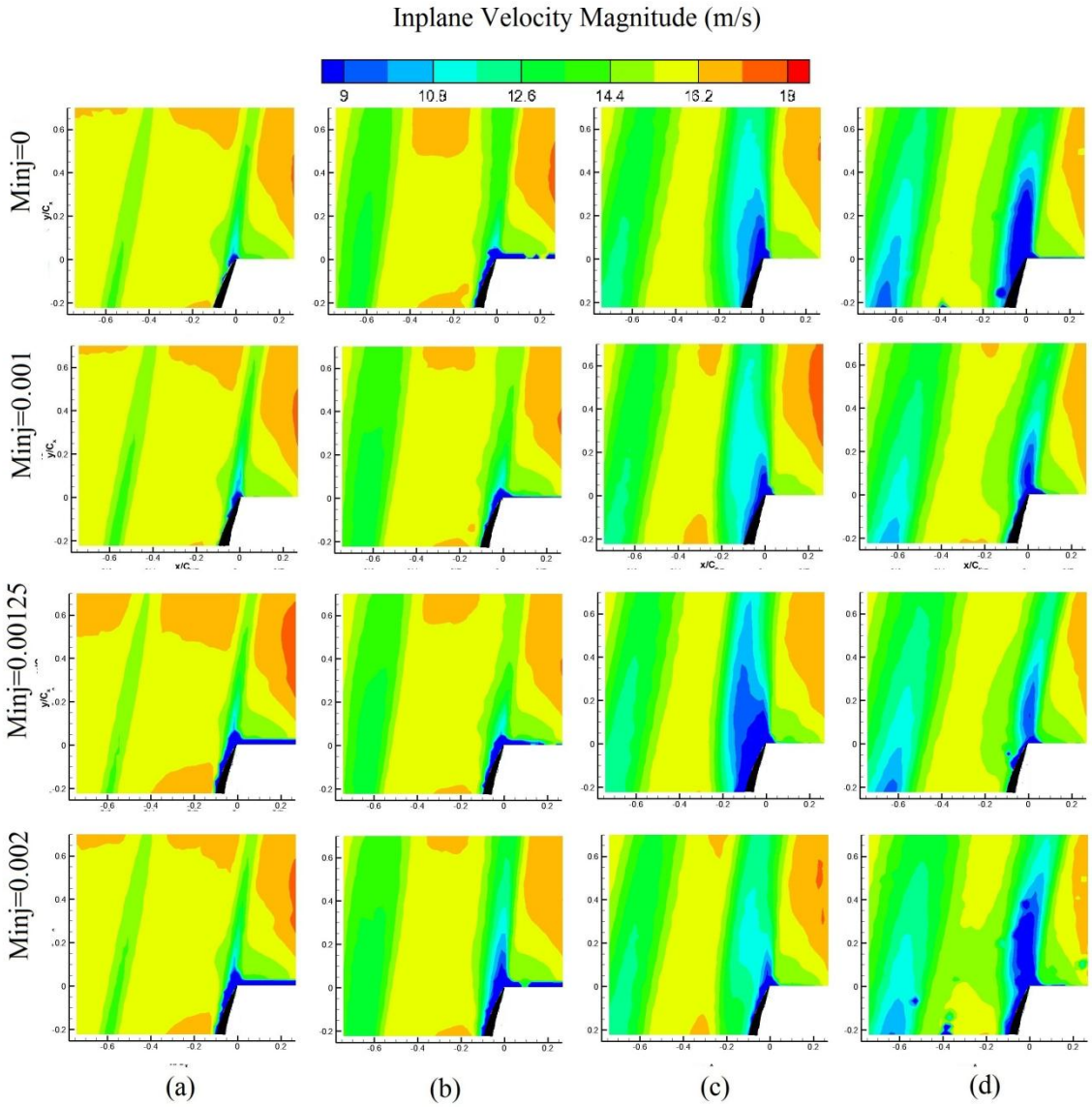

Figure 3.9 Inplane mean velocity magnitude contours for different injection mass flow rates at (a) 50% (b) 75% (c) 85% and (d) 95% span. Lower right hand corner is blocked by shadow. The black zone is the trailing edge of the test blade. The flow is from bottom to top

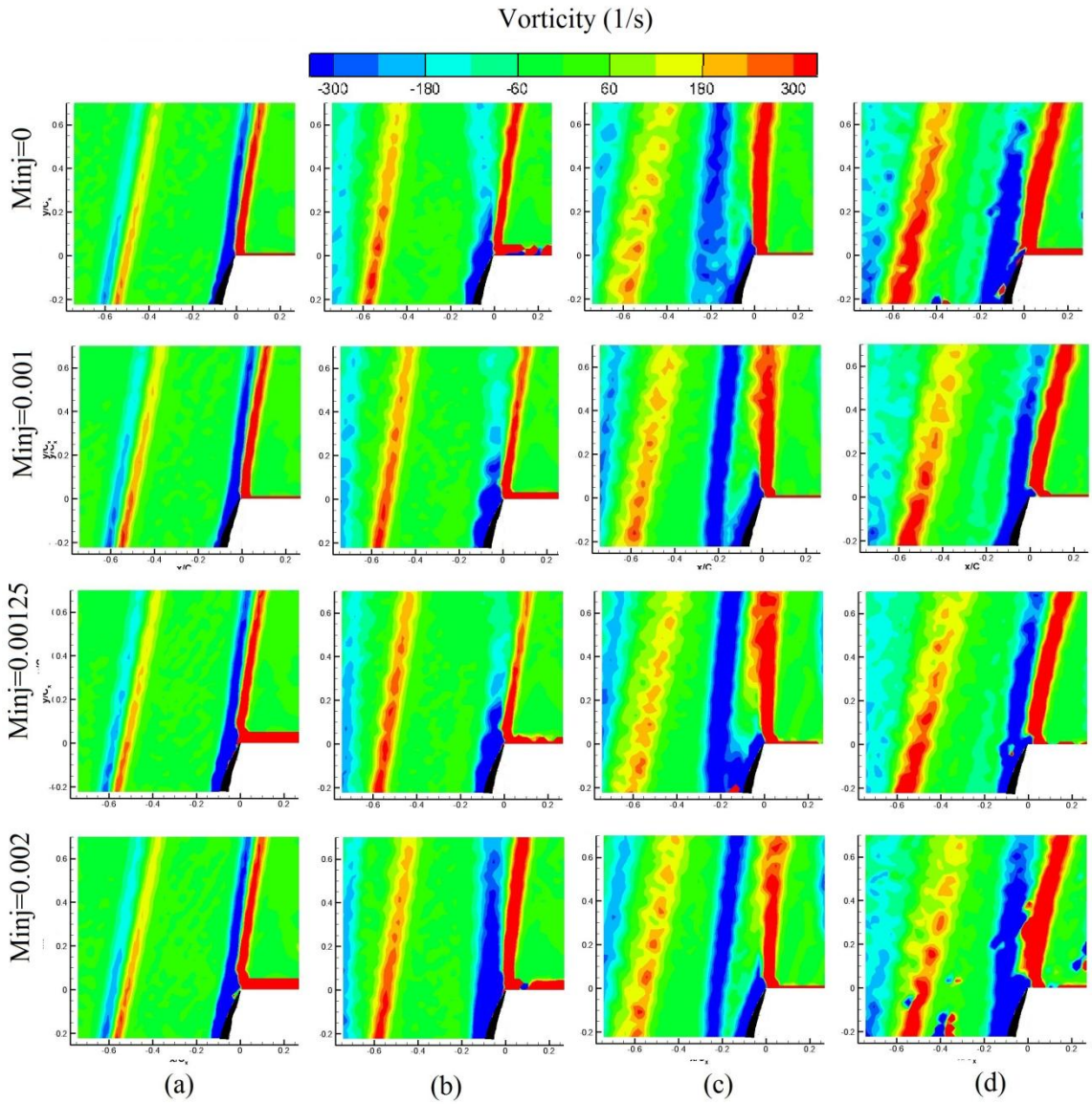

Figure 3.10 Mean vorticity (Ω_z) magnitude contours for different injection mass flow rates at (a) 50% (b) 75% (c) 85% and (d) 95% span. Lower right hand corner is blocked by shadow. The black zone is the trailing edge of the test blade. The flow is from bottom to top

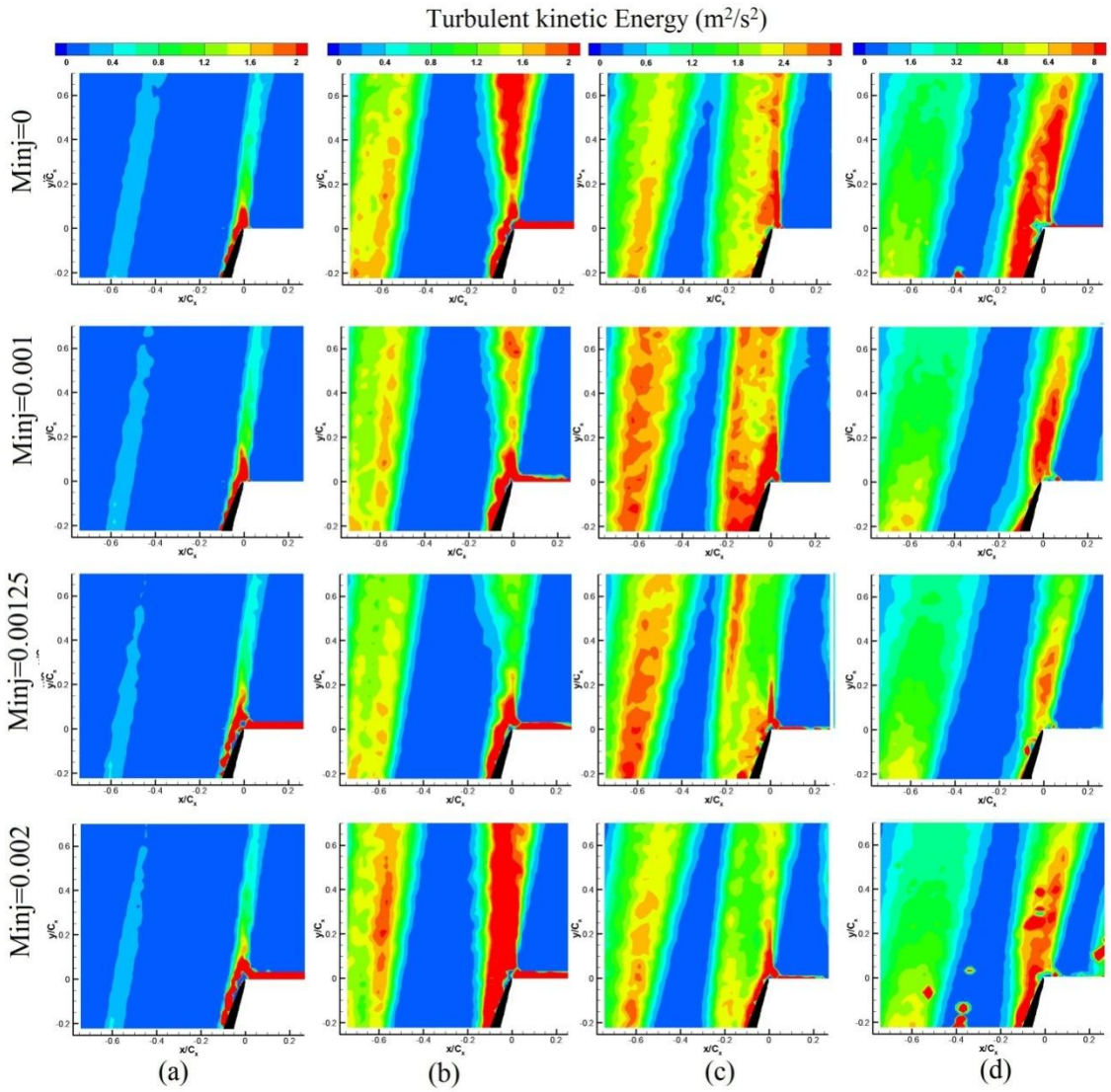

Figure 3.11 Turbulent kinetic energy contours for different injection mass flow rates at (a) 50% (b) 75% (c) 85% and (d) 95% span. Lower right hand corner is blocked by shadow. The black zone is the trailing edge of the test blade. The flow is from bottom to top

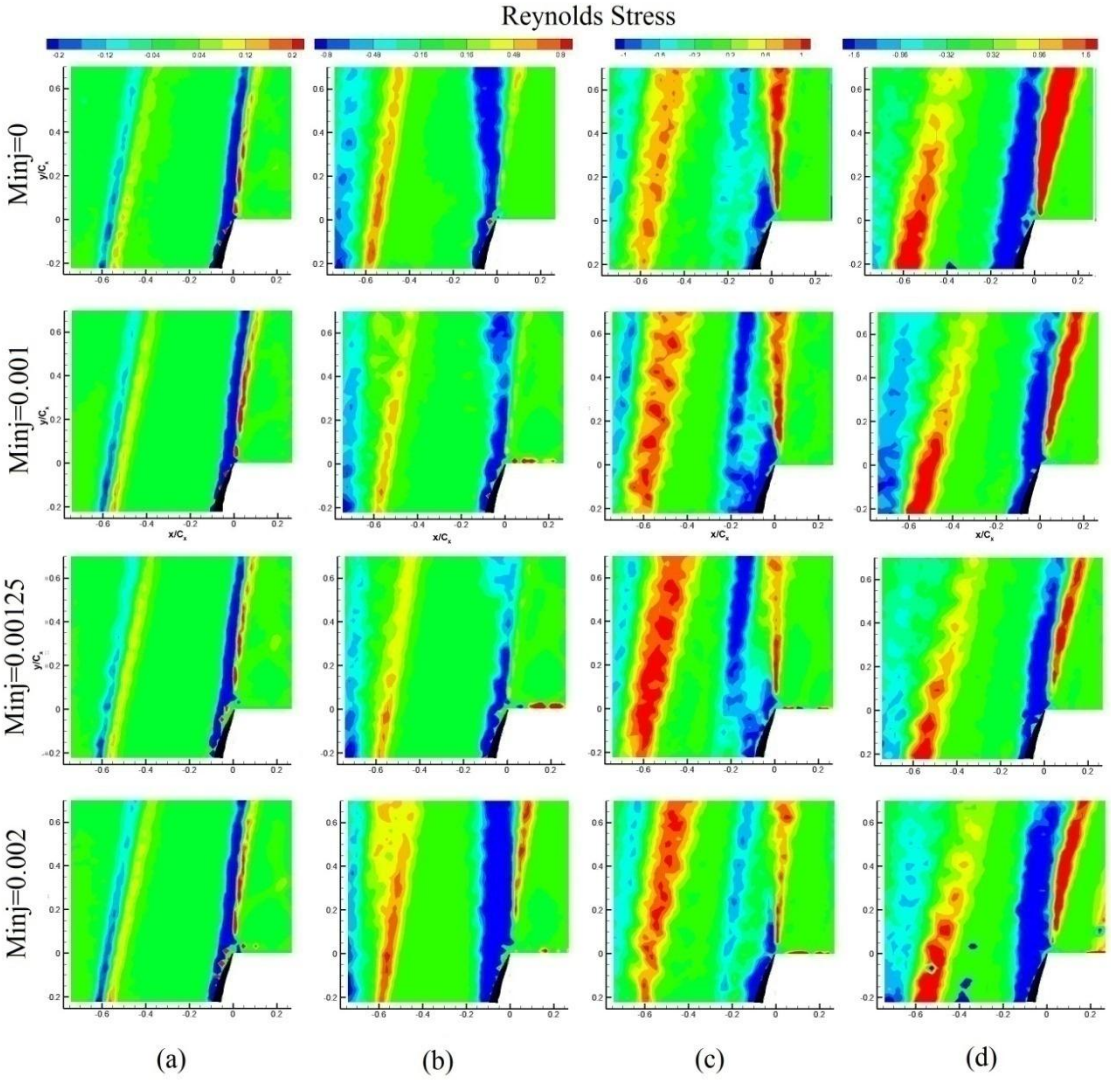

Figure 3.12 Reynolds shear stress contours for different injection mass flow rates at (a) 50% (b) 75% (c) 85% and (d) 95% span. Lower right hand corner is blocked by shadow. The black zone is the trailing edge of the test blade. The flow is from bottom to top

Figure 3.11 shows turbulent kinetic energy contours. Tip injection has a minimal effect at 50%, 75% and 85% spanwise location. But at 95% span, where leakage vortices are dominant, turbulence characteristics change with tip injection. All injection scenrios decrease the turbulence levels within the leakage wake. Again most effective injection case is the uniform waveform pattern when M_{inj}=0.00125. Figure 3.12 shows the Reynolds shear stress contour for different injection mass flow rates. Tip injection has no effect at 50% span location but at 75% span when M_{inj}=0.002, Reynolds shears within the wake seems to be increased by tip injection. Tip injection decreases the stress levels at 95% span. In all cases in the leakage wake of the test blade and the neighboring blade, Reynolds stress levels are decreased.

Figure 3.13 shows the wake center movement which is a result of the wake analysis (refer to section 3.1.2). It must be noted that when x_d value decreases, it means that the wake is less effective in the passage flow. At 50% span, tip injection has mior effects while at 75% span, uniform injection with M_{inj}=0.002 pushes the wake through the passage flow. At 85% span, all injection scenarios pushes the wake away from the suction side. At 95% span where the leakage vortices are dominant, uniform injection with M_{inj}=0.001 and M_{inj}=0.00125 moves the wake closer to the suction side which means leakage vortex is less dominant in passage mainstream flow.

Figure 3.14 presents the wake center velocities. As expected, tip injection does not have a major effect in wake center velocities at 50% and 75% span location but it must be noted that when M_{inj}=0.002, center velocity of the wake decreases which means that velocity defect in the wake zone is increased by tip injection. This result was also noted in previous paragraphs. At 85% span location, all injection scenarios increase the wake center velocity except M_{inj}=0.00125 case. Major effect of tip injection on wake center velocities can be seen at 95% span. All injection scenarios has a positive effect. When M_{inj}=0.00125, there is a velocity gain up to 35% compared to no injection case.

To explain the physical explanation of wake half-width, if the half-width of a wake is bigger this means that the size of the wake is bigger. Figure 3.15 shows the wake half-widths. As expected tip injection does mot have an effect on the size of the wake at 50% span. At 75% span it was previously noted that uniform injection with

M_{inj}=0.002 has a negative effect. This result can again be seen in wake half-width plots. At 85% span location, tip injection increases the size of the wake up to 0.2 axial chord downstream location. After that point, when there is a tip injection, size of the wake is less compared to no-injection case. At 95% span, where leakage vortices are dominant, all injection scenarios decrease the size of the wake. It must be noted that when M_{inj}=0.00125 there is a wake size reduction up to 30%.

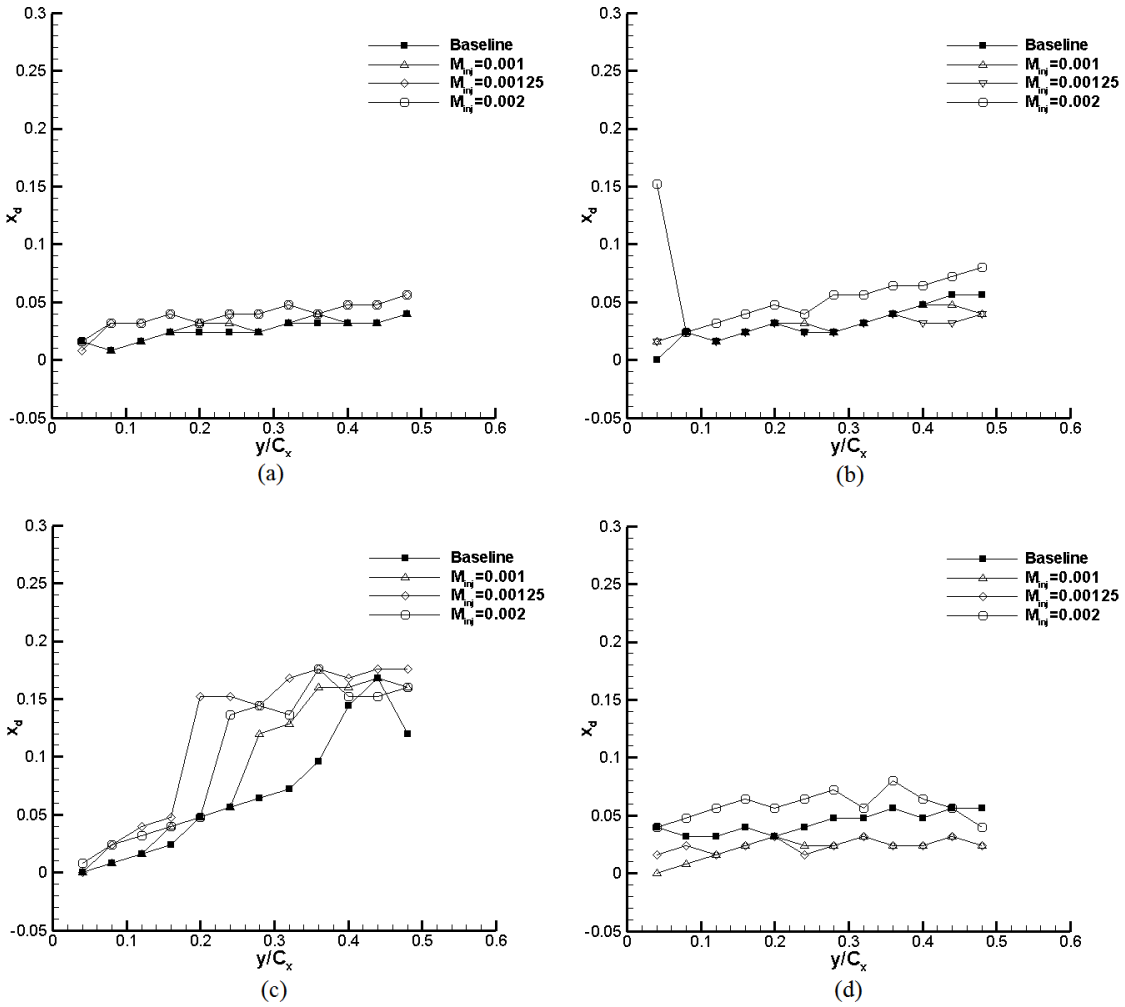

Figure 3.13 Wake center movements through streamwise direction for different injection mass flow rates at (a) 50% (b) 75% (c) 85% and (d) 95% span location

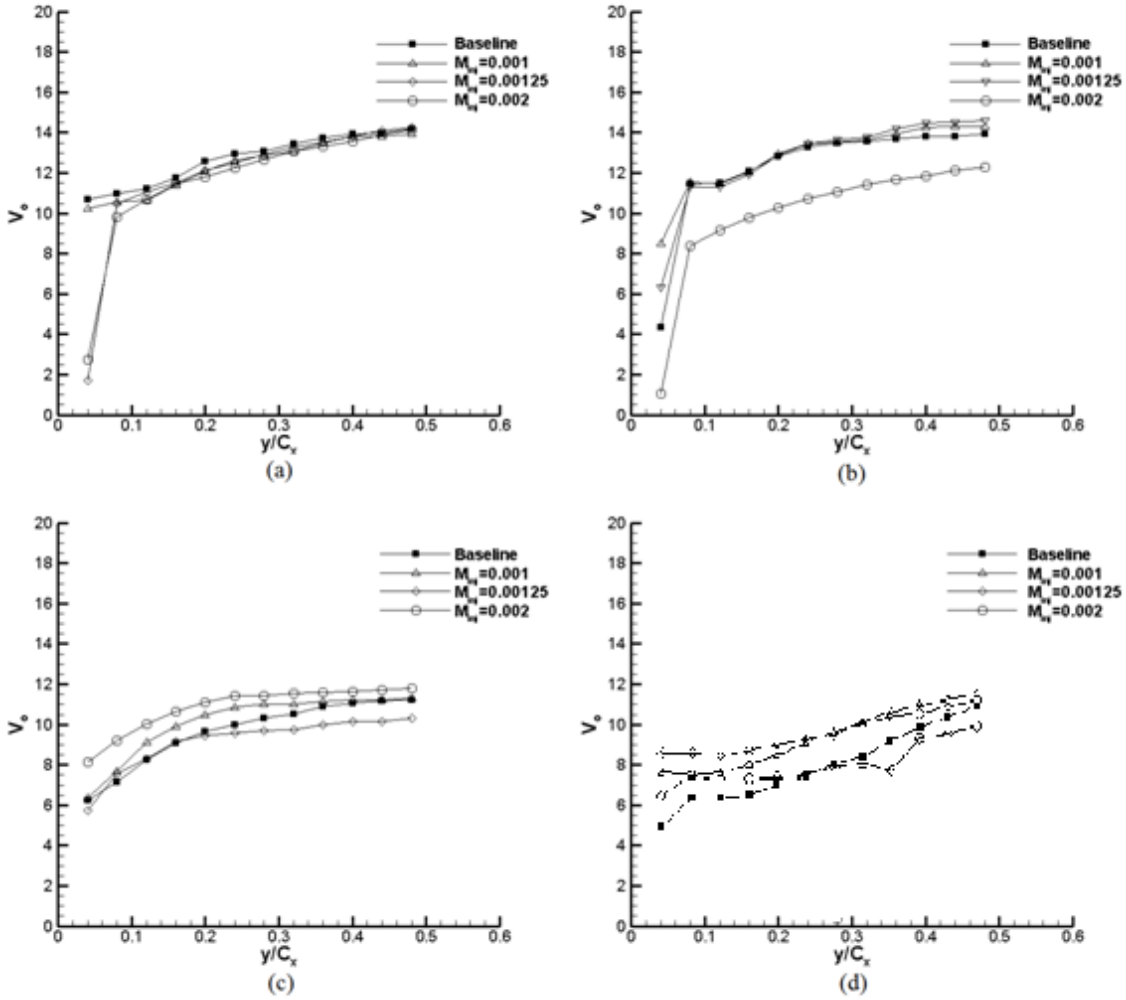

Figure 3.14 Wake center velocities through streamwise direction for different injection mass flow rates at (a) 50% (b) 75% (c) 85% and (d) 95% span location

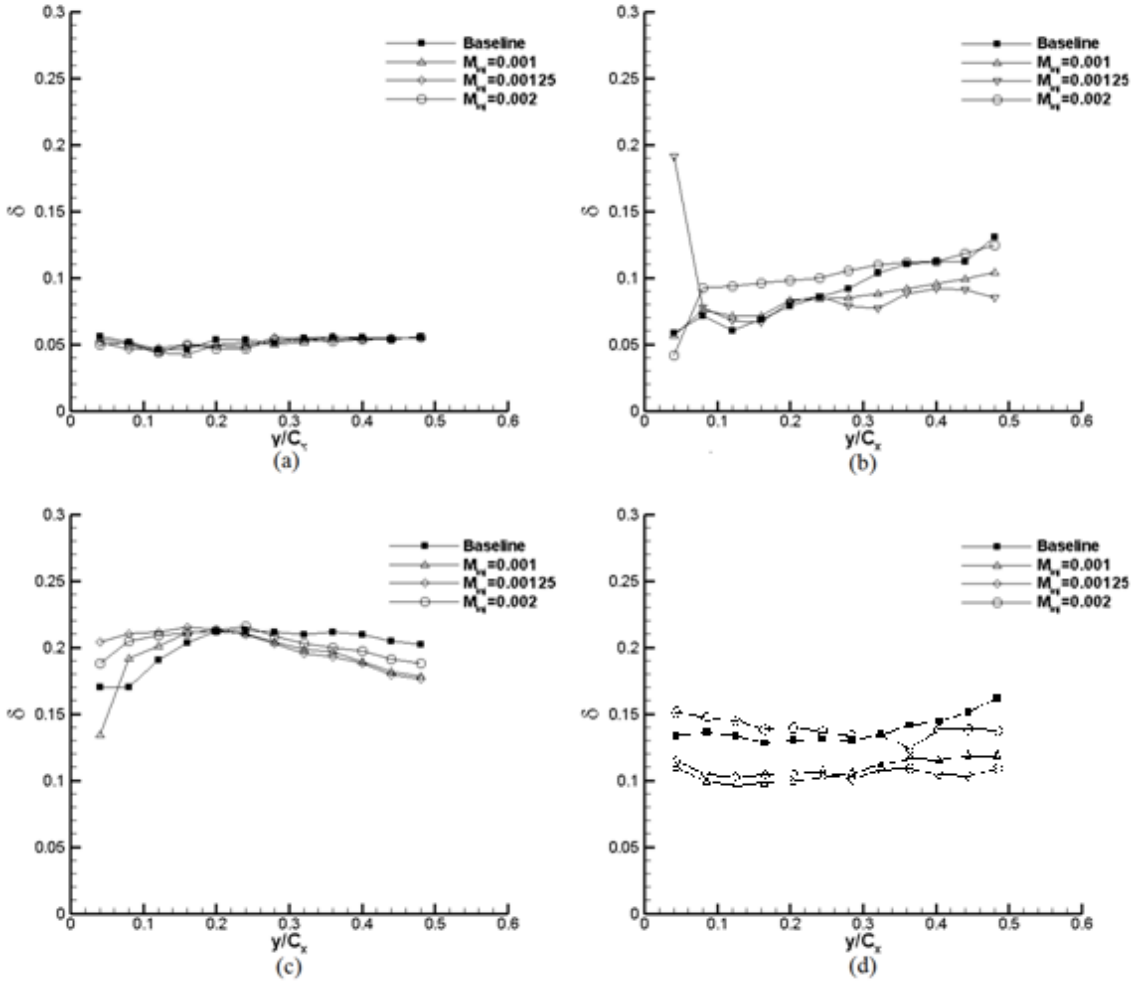

Figure 3.15 Wake half-widthsthrough streamwise direction for different injection mass flow rates at (a) 50% (b) 75% (c) 85% and (d) 95% span location

3.4 Effect of Injection Waveform Pattern

In order to investigate the effect of waveform injection, four different waveform injection patterns are generated along the camberline at the tip of the test blade. These are triangular, reversed-triangular, half-sine and reversed half-sine patterns. The results of these measurements are compared to the no-injection baseline case as well as to the corresponding uniform injection cases, which have the same average mass injection ratio.

3.4.1 Effect of Injection Waveform Pattern at M_{inj}=0.001

Figure 3.16 shows the measured total pressure loss coefficient contours 0.5 axial chords downstream of the blade row, covering a region between 85% to 100% span, for no-injection, reversed-triangular, triangular and uniform injection cases. Keep in mind that the triangular and the uniform injection cases all have the same average mass injection ratio. The blue-green contour regions correspond to the wakes downstream of the two of the blades in the cascade. The blade on the right-hand-side is the injection test blade whereas no injection takes place from the blade on the left.

One can observe that the triangular injection pattern is not as effective as the reversed triangular or uniform patterns in terms of loss reduction when compared to the no-injection baseline case. The most reduction in total pressure loss levels are observed for the reversed triangular pattern. The pressure losses within the leakage region seem to get considerably reduced when compared to the no-injection case.

When one compares the reverse triangular injection pattern with corresponding uniform injection case, the reverse waveform injection case seem to create similar levels of reduction in total pressure loss levels above 90% span but more reduction is observed below 90% span. Keeping in mind that both injection patterns have the same average mass injection ratio, one can observe that the influence of reversed triangular injection pattern get more pronounced within the wake region. Therefore one can conclude that the injection waveform pattern could have an impact on the total loss characteristics of the blade when appropriately selected. This is of course

mainly due to the leakage characteristics of the blade and if the injection waveform pattern is chosen to be consistent with those characteristics, one can achieve more reduction in total loss levels. Note that the effect of waveform injection on the adjacent blade seems to be minimal as can be seen in Figure 3.16.

Figures 3.17 shows the pitchwise total pressure loss coefficient variations at 95% and 85% span for triangular injection patterns. Again, the results are compared with the no-injection and corresponding uniform injection cases. At 95% span (Figures 3.17.a), low total pressure region seems to get reduced when the triangular pattern is applied, however, the levels are not as reduced as the corresponding uniform injection case. On the other hand, the total pressure loss reduction of the reversed triangular case is about the same as the uniform injection case. At 85% span, however, the uniform mass injection creates deeper wake zones when compared to any of the waveform injection cases. This may indicate that when reversed waveform injection is applied, the leakage losses get reduced similar to the case of uniform injection, however, the blade loading and hence the wake deficits do not get affected much and the levels stay close to that of the no-injection case.

Figures 3.18 shows pitch averaged total pressure loss coefficient variations for triangular injection patterns. At first it can be seen that all injection patterns reduce the pressure loss within the leakage vortex region. Triangular injection is the least efficient case. Most pressure gain is investigated in uniform injection. But uniform injection does not have a pressure gain in passage vortex region. Triangular injection is the most effective injection scenario for the passage vortex region.

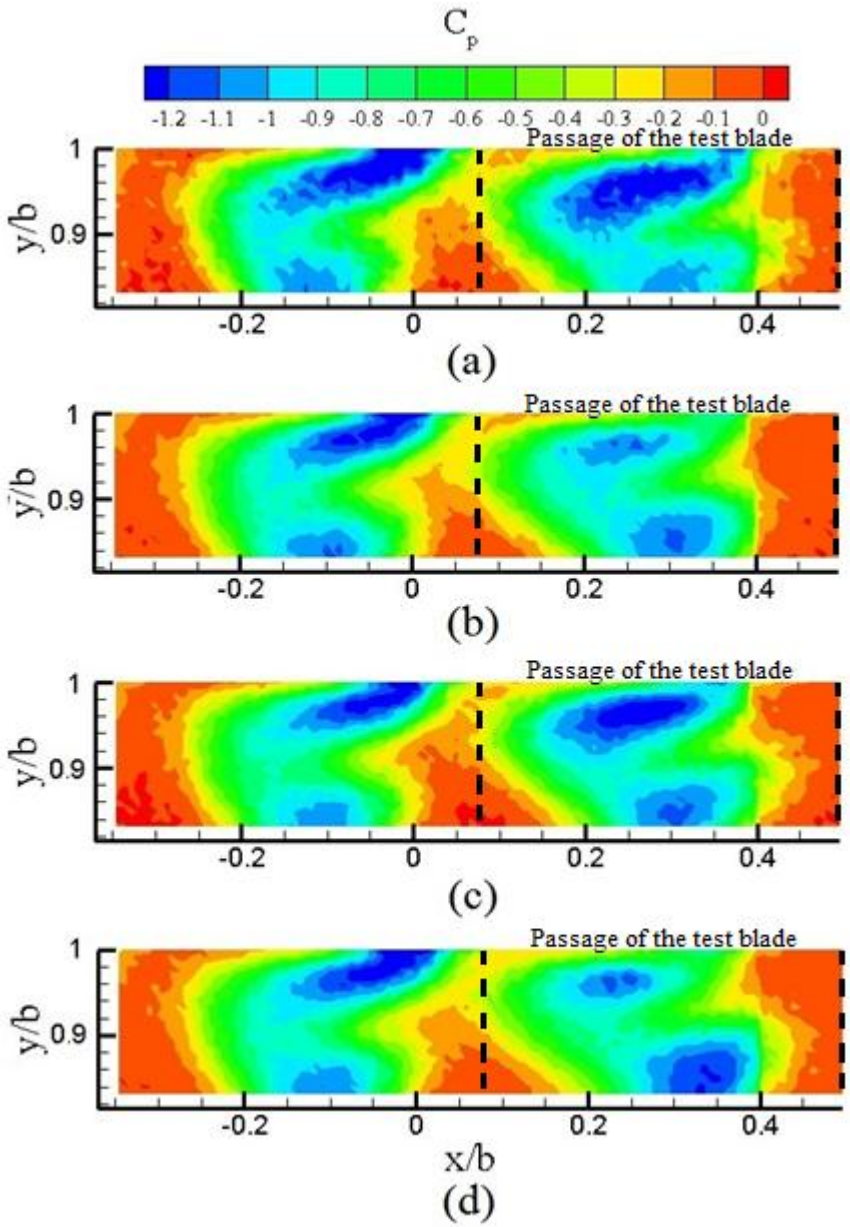

Figure 3.16 Measured total pressure loss coefficient contours 0.5 axial chords downstream of the blade row for three different injection waveforms all having M_{inj} = 0.001 and comparison with the no-injection case. (a) No injection (b) Reversed Triangular (c) Triangular (d) Uniform

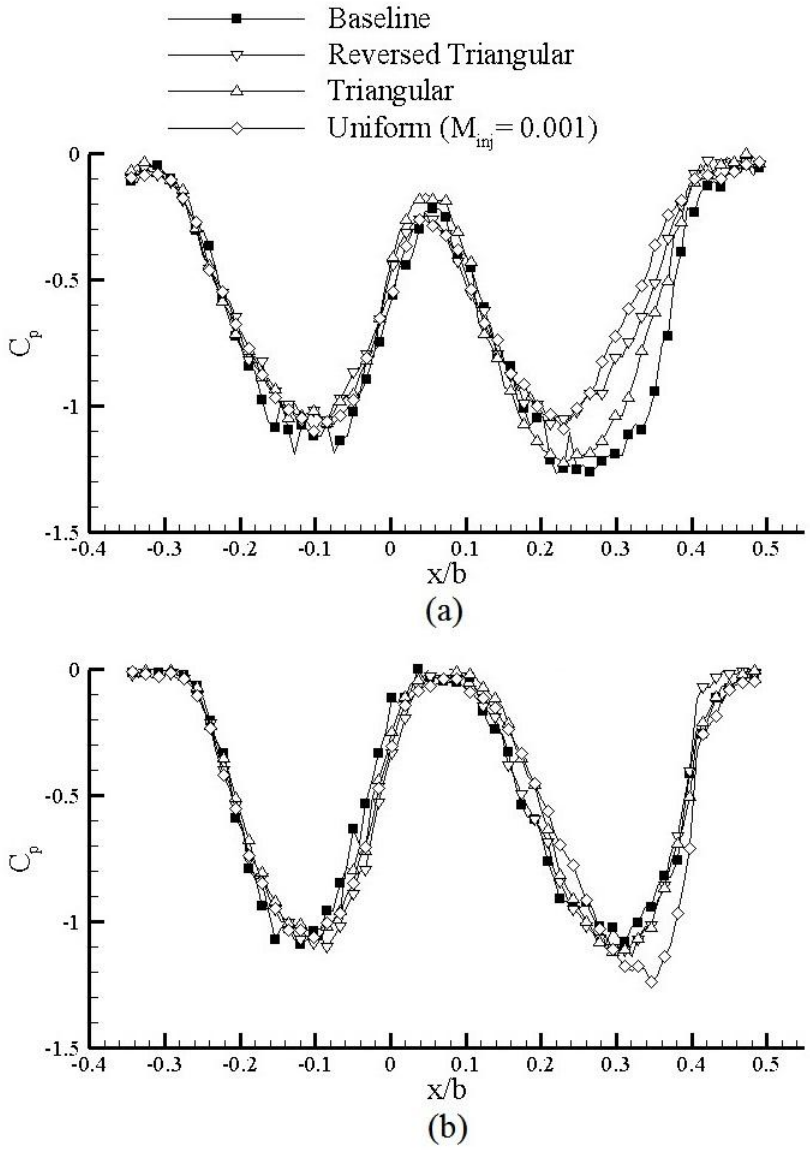

Figure 3.17 Pitchwise total pressure loss coefficient variations at (a) y/b=0.95 and (b) y/b=0.85 for three different injection waveforms and comparison with the no-injection case. All have M_{inj} = 0.001

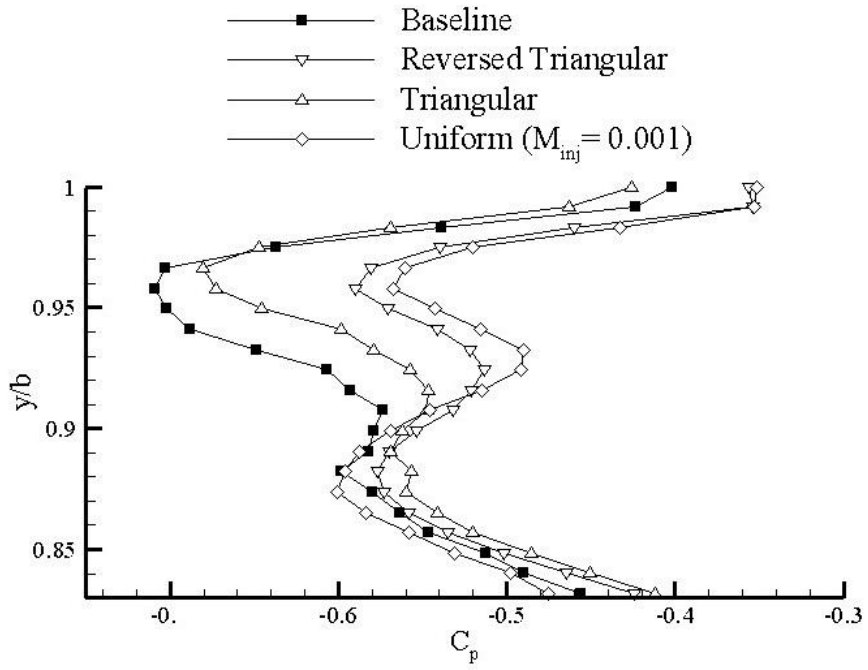

Figure 3.18 Pitch averaged total pressure loss coefficient variations for three different injection waveforms and comparison with the no-injection case. All have M_{inj} = 0.001

Table 3.2 presents the passage averaged total pressure loss coefficients using pitch averaged total pressure loss coefficients and passage boundaries shown in Figure 3.16. Passage averaged total pressure loss coefficients combine the pressure loss levels within the passage vortex zone and leakage vortex zone. As can be seen highest amount of reduction occurs in the case of reversed-triangular injection pattern and it's followed by the uniform injection. The triangular injection has the lowest amount of loss reduction among all waveforms. In triangular injection case, it was noted that pressure reduction in leakage vortex zone is minimal. Reversed triangular and uniform injection scenarios can block the inlet boundary layer to enter the gap, but in triangular injection, inlet boundary layer is not blocked and enters the gap which creating a leakage vortex before 30% chord of the gap. These results are also presented by Mercan et al. [23].

Table 3.2 Passage averaged total pressure loss coefficients and pressure loss reduction levels for different waveforms and comparison with the no injection case. All have M_{inj}=0.001

M_{inj}	Waveform Pattern	C_{μ}	$C_{p,passage}$	Pressure Loss Reduction (%)
0	Baseline	0	-0.578	0
0.001	Reversed Triangular	0.055	-0.516	10.695
0.001	Triangular	0.055	-0.552	4.485
0.001	Uniform	0.039	-0.518	10.281

Figure 3.19 shows the inplane velocity magnitudes. First observation is that the wake zones of two of the blades can be clearly identified by diagonally extending low momentum regions downstream of the blades, especially for 50% span for all injection cases. On this plane, the effect of tip injection seems to be minimal on the wake structureas well as 75% span. On 85% and 95% planes, the effects of the tip leakage flow and vortex start to dominate the wake, and wider low momentum areas are generated. However, the width, the shape and the extent of these areas change with each injection scenario. In all cases and in both 85% and 95% span planes, the low momentum region gets narrower and the extent of the lowest momentum region seems to get shorter in the presence of injection.

There are also differences between waveform patterns. For example the reversed triangle case has a bigger velocity defect in the near wake compared to the triangular and the uniform injection cases. The uniform injection seems to be the most effective such that for example at 95% span the leakage seems to be significantly reduced with a much shorter and narrower wake zone compared to the no-injection case. These results are also supported by the mean vorticity (Ω_z) magnitude contours presented in Figure 3.20. The shape and the width of the wake gets affected in a different characteristic depending on the injection waveform shape. It must be noted that for midspan measurements, the flow is periodic and the neighboring blade is not affected significantly by the tip injection.

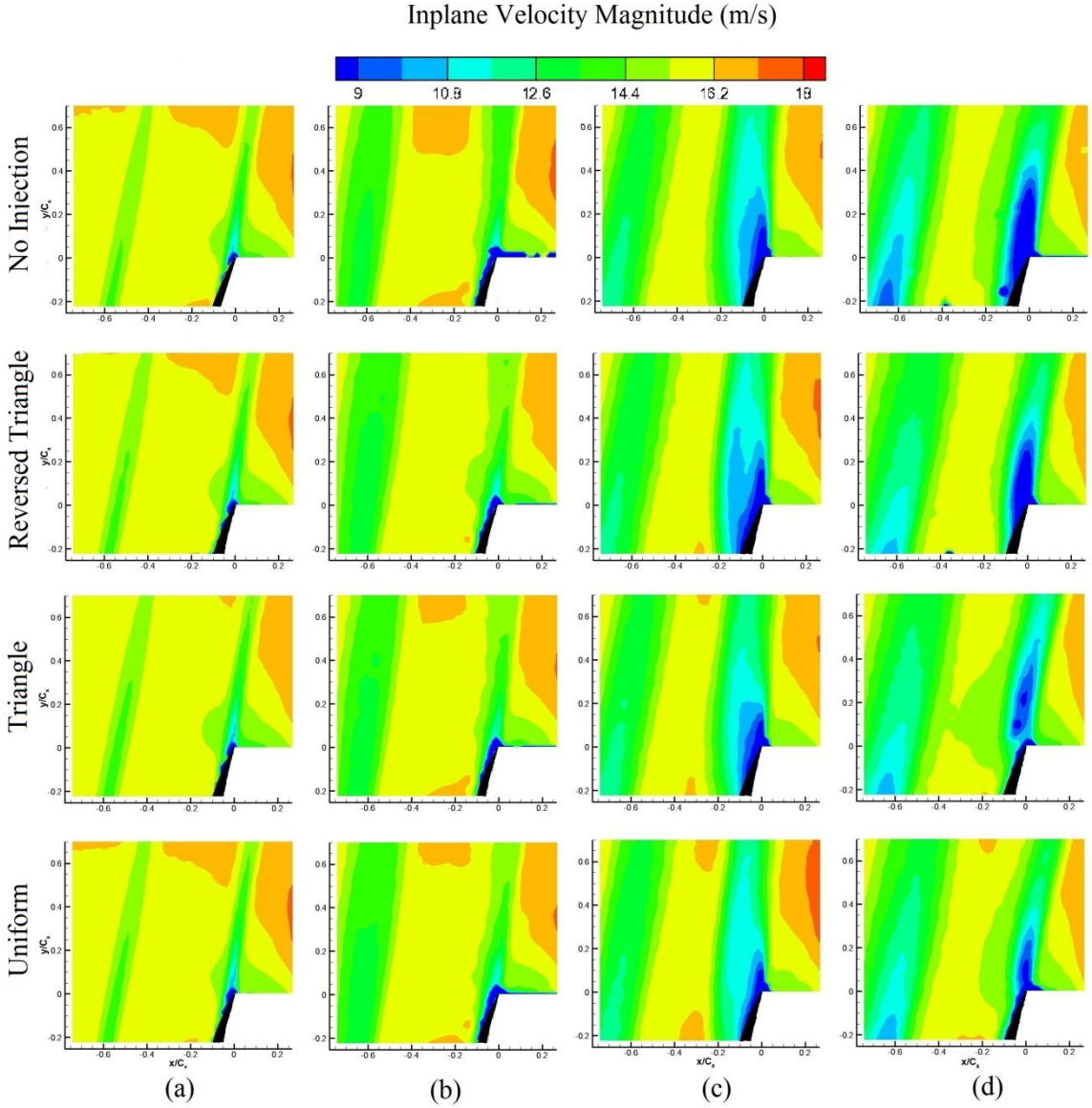

Figure 3.19 In-plane mean velocity magnitude contours for different injection waveform patterns where M_{inj}=0.001 at (a) 50% (b) 75% (c) 85% and (d) 95% span. Lower right hand corner is blocked by shadow. The black zone is the trailing edge of the test blade. The flow is from bottom to top

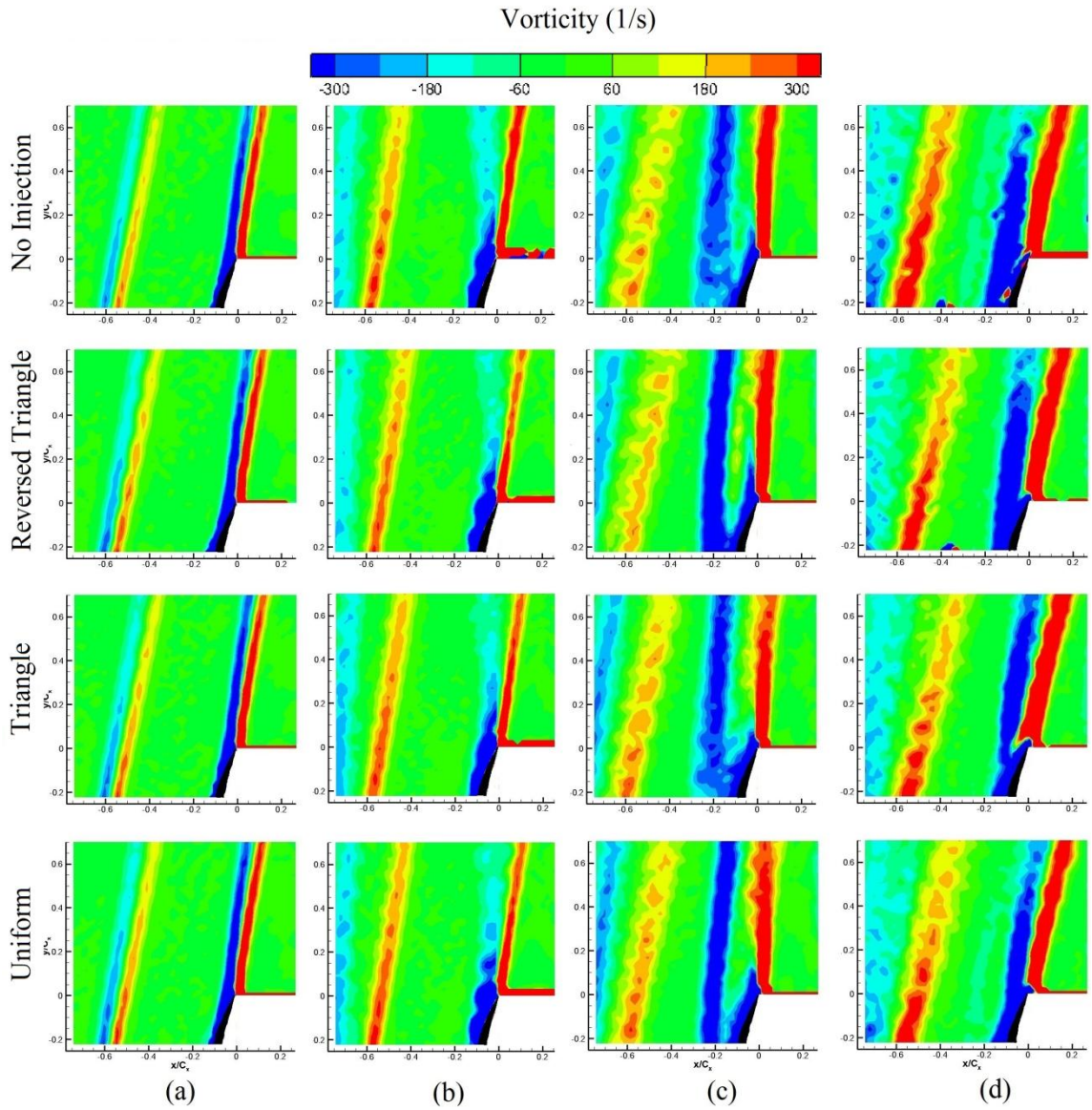

Figure 3.20 Mean vorticity (Ω_z) magnitude contours for different injection waveform patterns where M_{inj}=0.001 at (a) 50% (b) 75% (c) 85% and (d) 95% span. Lower right hand corner is blocked by shadow. The black zone is the trailing edge of the test blade. The flow is from bottom to top

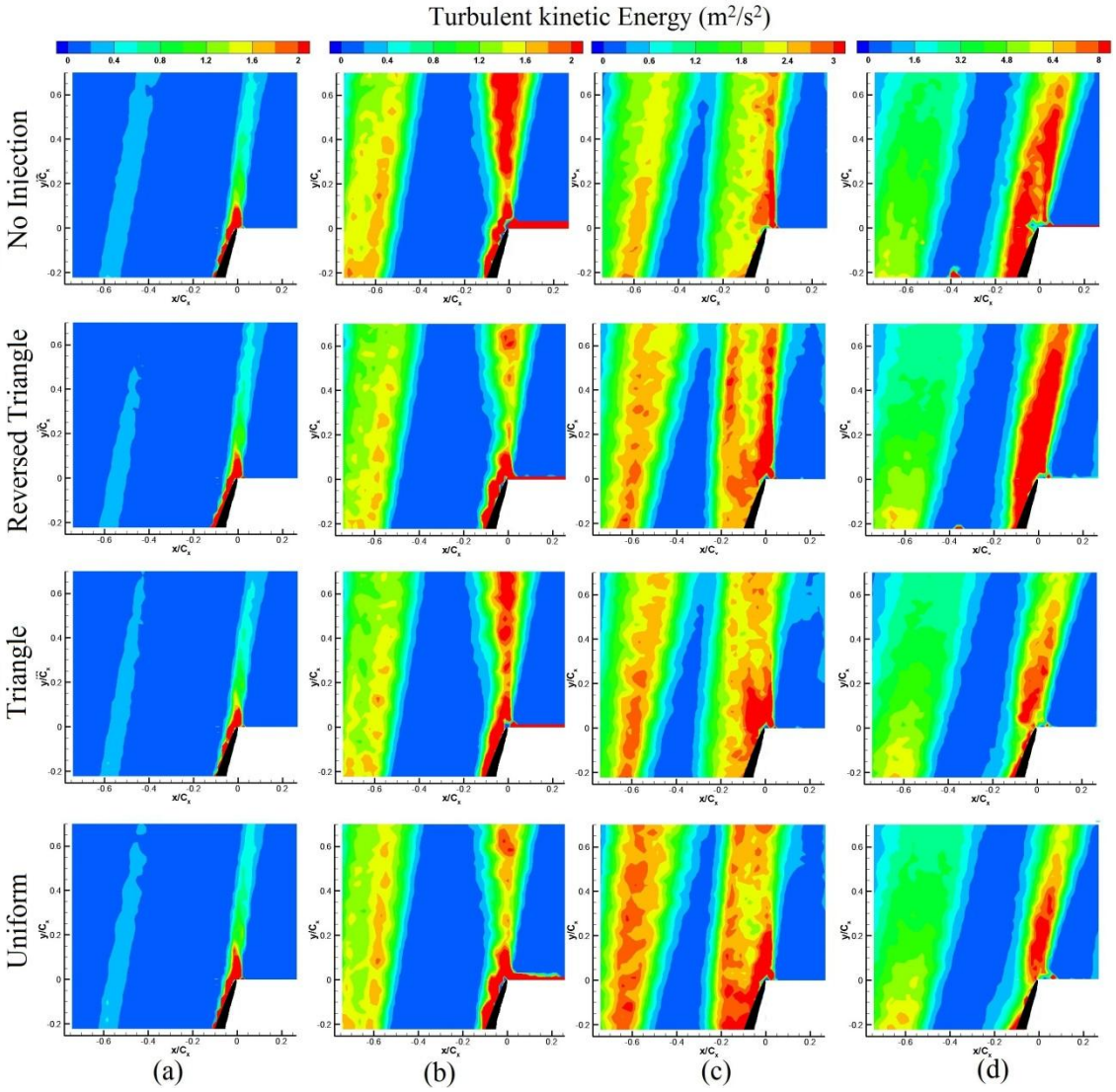

Figure 3.21 Turbulent kinetic energy contours for different injection waveform patterns where M_{inj}=0.001 at (a) 50% (b) 75% (c) 85% and (d) 95% span. Lower right hand corner is blocked by shadow. The black zone is the trailing edge of the test blade. The flow is from bottom to top

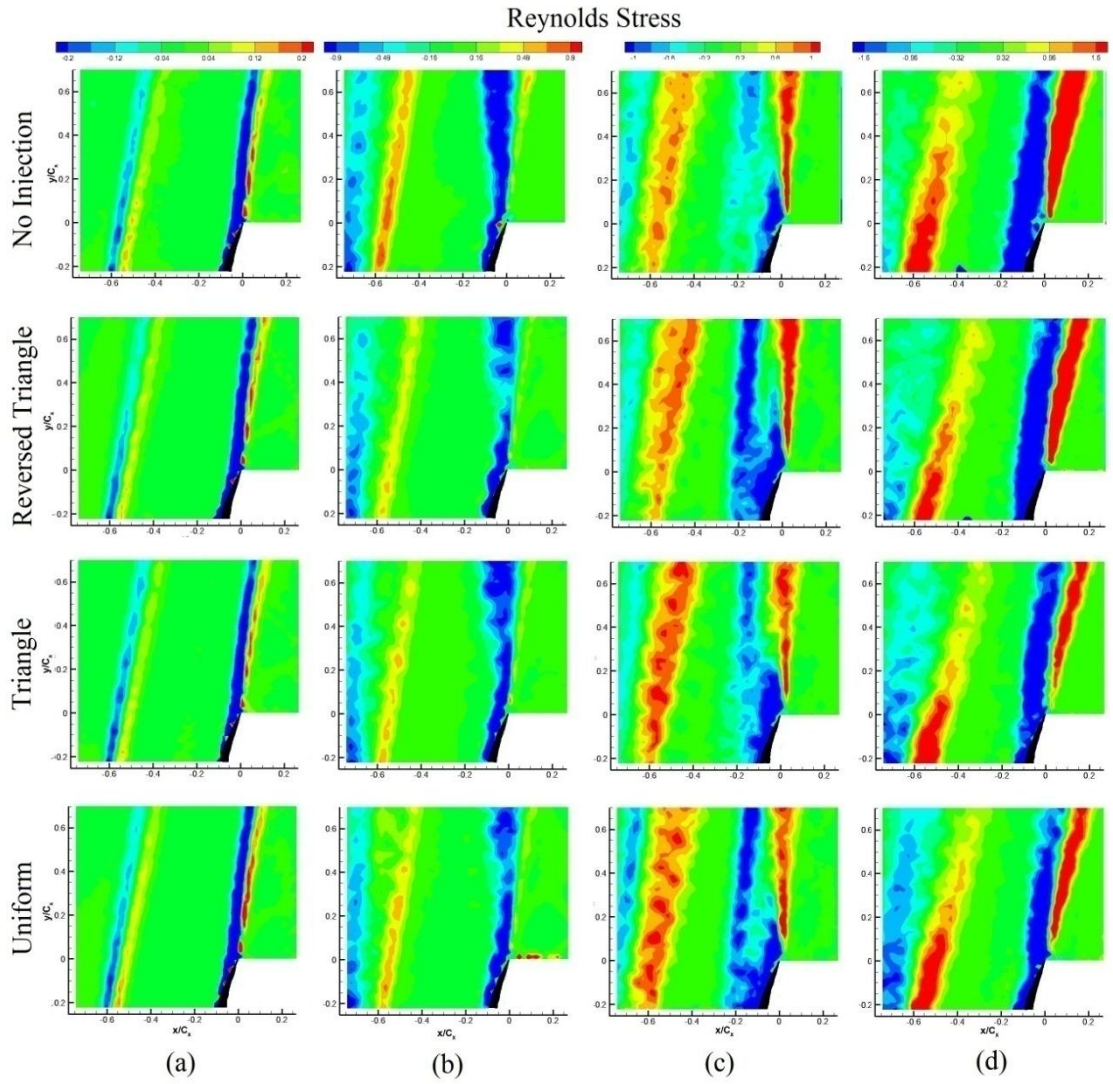

Figure 3.22 Reynolds shear stress contours for different injection waveform patterns where M_{inj}=0.001 at (a) 50% (b) 75% (c) 85% and (d) 95% span. Lower right hand corner is blocked by shadow. The black zone is the trailing edge of the test blade. The flow is from bottom to top

Figure 3.21 shows the turbulent kinetic energy contours for the same spanwise locations and injection cases as in Figures 3.19 and 3.20. The wake regions are again identified this time as diagonally extending elevated turbulent kinetic energy regions. The effects on 50% and 75% plane again are minimal. Tip injection does not seem to have a significant effect on the elevated turbulent kinetic energy region situated between $-0.3<x/C_x<0$ on the 85% span plane (Figure 3.21.c). However, the turbulence characteristics do get affected by injection substantially at 95% span plane (Figure 3.21.d). High levels of turbulence that cover a wide area in the case of no-injection sequentially get reduced when the injection goes from reversed-triangular to triangular to uniform. Again the uniform seems to have the biggest impact on the width and extent of the high turbulent wake zone. In fact it looks like that the leakage effects are minimized and the turbulent wake itself gets much more identifiable at 95% span.

Figure 3.22 presents the Reynolds shear stress distributions. As expected wake regions show up as positive and negative layers of shear stress. At 85% span, which is most probably within a passage vortex zone as depicted from the total pressure measurements, this positive-negative distribution characteristic seems to get distorted with injection, especially near the trailing edge. Interestingly enough at a higher spanwise location like 95% this pattern still persists and the effect of injection seems to be only towards reducing the width of the wake zone. No significant distortions are observed.

Figure 3.23 shows the wake center movements. as mentioned before, tip injection has no effect on wake structures at 50% and 75% span plane. At 85% span, in first sight there seems that all injection scenarios increase the displacement of the wakes. but it must be noted that when there is injection velocity defect within the wake quickly diminishes (Figure 3.19.c). At 95% span, where leakage flow is dominant, all injection scenarios decrease the movement of the wake and moves the wake through the suction side of the blade.

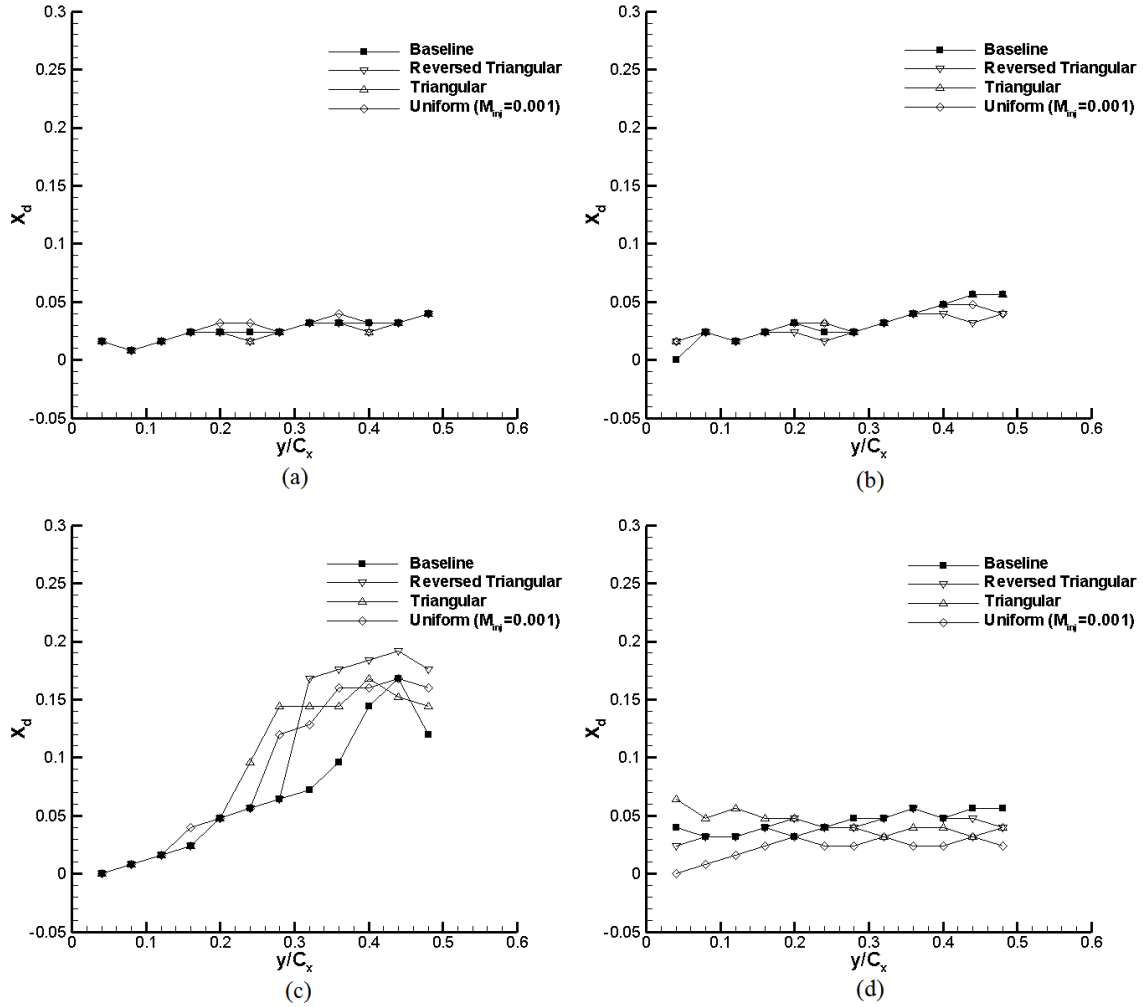

Figıre 3.23 Wake center movements through streamwise direction for different injection waveform patterns where M_{inj}=0.001 at (a) 50% (b) 75% (c) 85% and (d) 95% span location

Figure 3.24 presents the wake center velocities. At 50% and 75% span tip injection does not affect the velocity profile within the wake zone. At 85% reversed-triangular and uniform injection patterns have a wake center velocity gain about %10 of no injection wake. But it seems that when there is triangular waveform injection, wake center velocity decreases near the trailing edge. At 95% span all injection scenarios increase the wake center velocity up to 0.3 axial chord downsteam. After that point, triangular injection loses its efficiency. Also it can be noted that uniform injection it the most efficient case, there is a 20% velocity gain at the wake centers.

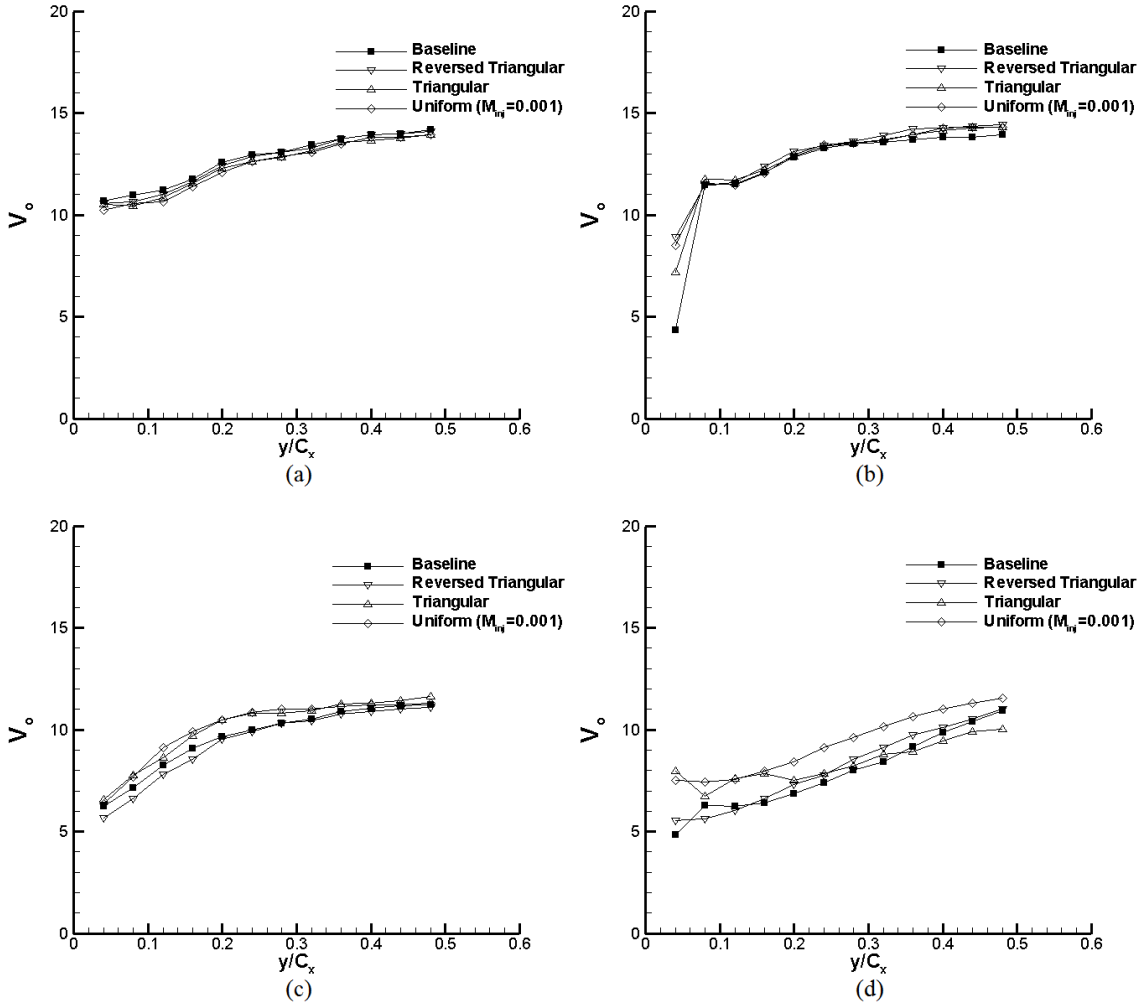

Figure 3.24 Wake center velocitiesthrough streamwise direction for different injection waveform patterns where M_{inj}=0.001 at (a) 50% (b) 75% (c) 85% and (d) 95% span location

Figure 3.25 shows the wake half-widths for different injection waveform patterns.at 75% span, where the flow is a combination of passage vortex and wake of the blade, tip injection decreases the size of the wake. At 85% span up to 0.2 axial chord downstream location, all injection waveforms increase the size of the wake. But after that point uniform waveform pattern has a positive effect on the size of the wake. At 95% span, all injection scenarios decrease the size of the vortex. Triangular pattern seems to be less effective than reversed-triangular pattern by means of decreasing the size of the wake. For all these cases, uniform waveform is the most effective pattern which is creating a decrease of wake size up to 30%.

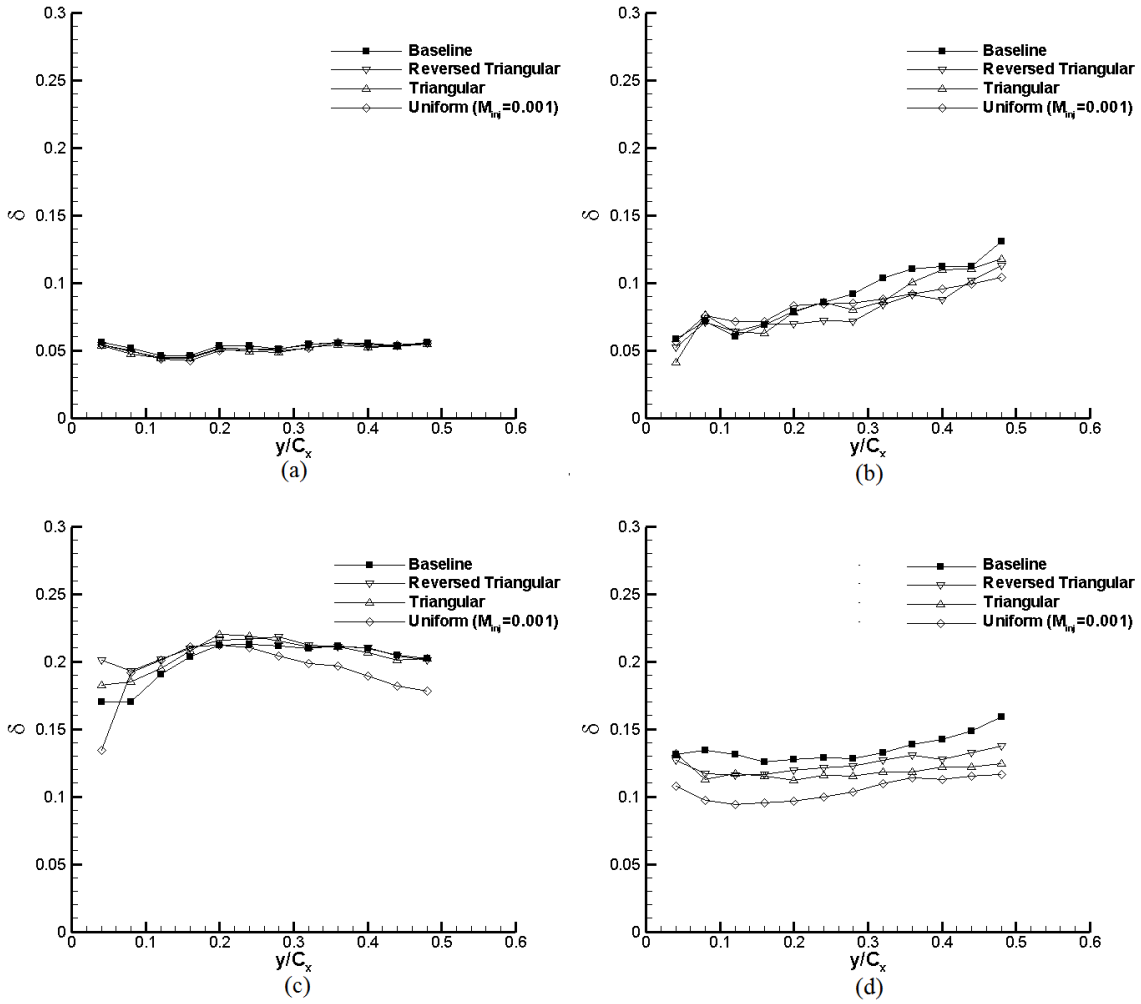

Figure 3.25 Wake half-widths through streamwise direction for different injection waveform patterns where M_{inj}=0.001 at (a) 50% (b) 75% (c) 85% and (d) 95% span location

3.4.2 Effect of Injection Waveform Pattern at M_{inj}=0.00125

To understand the effects of injection waveform pattern on tip leakage characteristics, another waveform set is organized at different injection mass flow rate. Reversed half-sine, sine and corresponding uniform waveforms are investigated all having an injection mass flow rate Minj=0.00125. Figure 3.26 presents the measured total pressure loss coefficients. It can easily be concluded that tip injection decreases the pressure loss within the leakage zone. Half-sine waveform is less efficient while reversed half-sine and uniform waveform has similar effects. Also, passage vortex zone of the test blade is affected. With uniform injection pressure loss

within the passage vortex zone is increased. Also it must be noted that leakage vortex of the neighboring blade gets smaller and moves through the endwall.

Pitchwise total pressure loss coefficient variations at 95% and 85% span are presented in Figure 3.27. It can be seen that tip injection decreases total pressure loss within the leakage vortex zone, also the vortex moves through the suction side of the test blade. Reversed half-sine and uniform injection waveform patterns have similar effects. All injection scenarios create a pressure gain within the leakage zone of the neighboring blade. At 85% span (Figure 3.27.b), injection does not have a major effect on wake structures but uniform waveform creates a pressure drop within the passage vortex zone of the test blade. In Figure 3.28, pitch averaged total pressure loss coefficients for the test blade are presented. For the leakage vortex region, half-sine waveform does not change the pressure levels significantly but moves the vortex through the endwall. Uniform and reversed half-sine waveforms have similar effects. At the passage vortex region, uniform injection increases the total pressure loss levels. Both half-sine and reversed half-sine waveforms create a pressure gain about 10% compared to no-injection case.

Table 3.3 presents the passage averaged total pressure loss coefficients using pitch averaged total pressure loss coefficients and passage boundaries shown in Figure 3.26. Passage averaged total pressure loss coefficients combine the pressure loss levels within the passage vortex zone and leakage vortex zone. Reversed half-sine waveform creates a pressure gain within the passage up to 14% compared with no injection case, while uniform and half-sine waveforms are not effective as reversed half-sine.

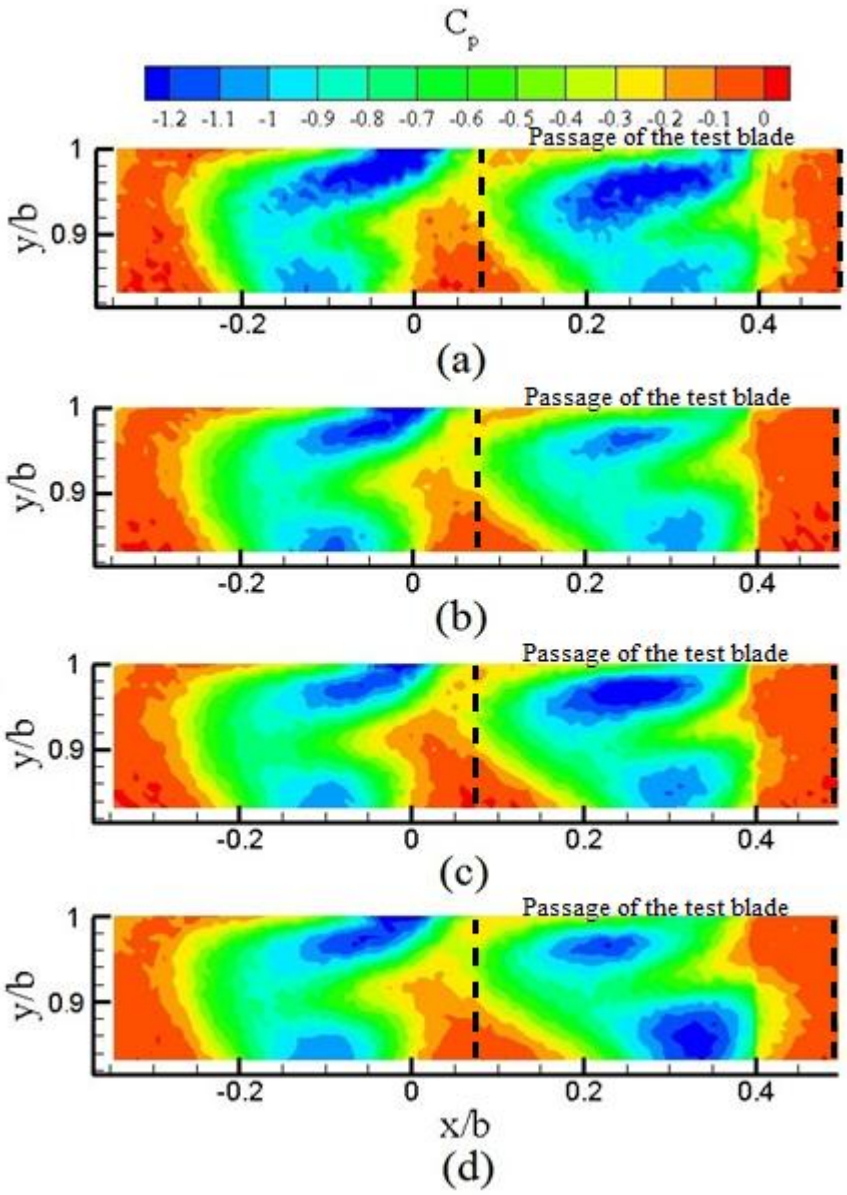

Figure 3.26 Measured total pressure loss coefficient contours 0.5 axial chords downstream of the blade row for three different injection waveforms all having M_{inj} = 0.00125 and comparison with the no-injection case. (a) No injection (b) Reversed Half-Sine (c) Half-Sine (d) Uniform

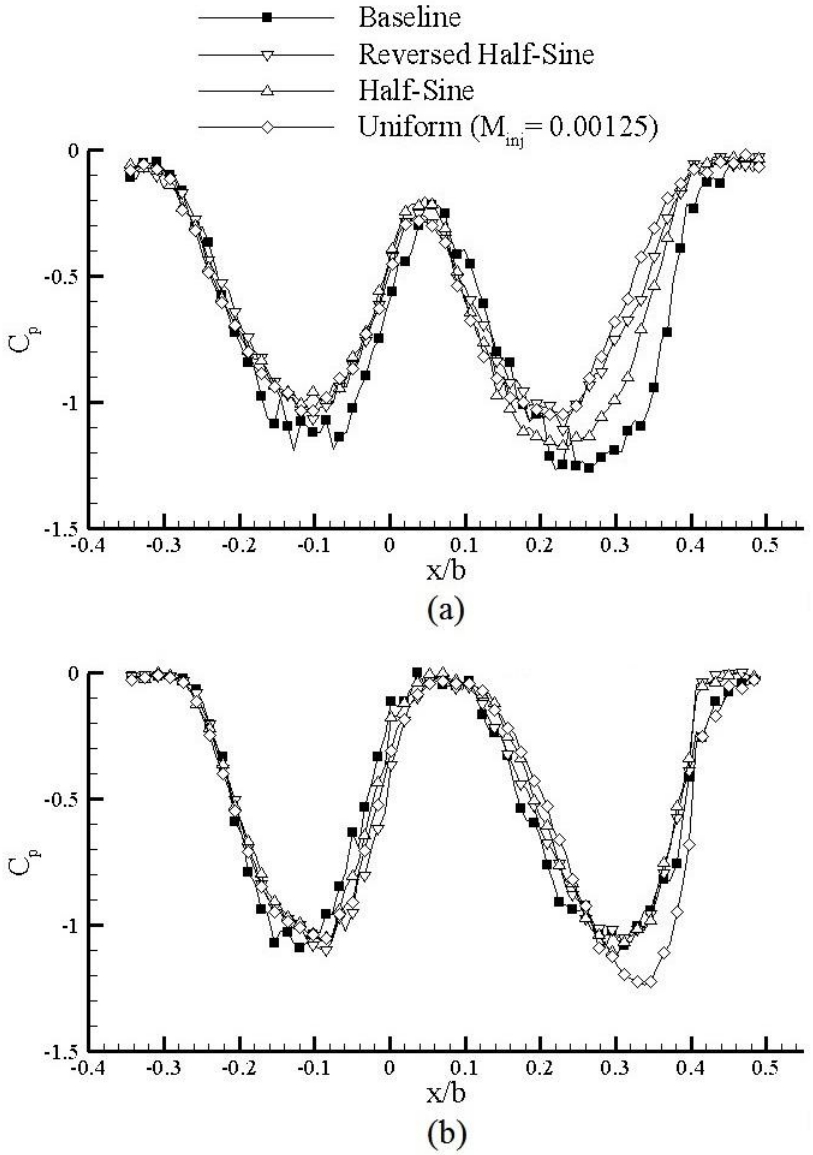

Figure 3.27 Pitchwise total pressure loss coefficient variations at (a) y/b=0.95 and (b) y/b=0.85 for three different injection waveforms and comparison with the no-injection case. All have M_{inj} = 0.00125

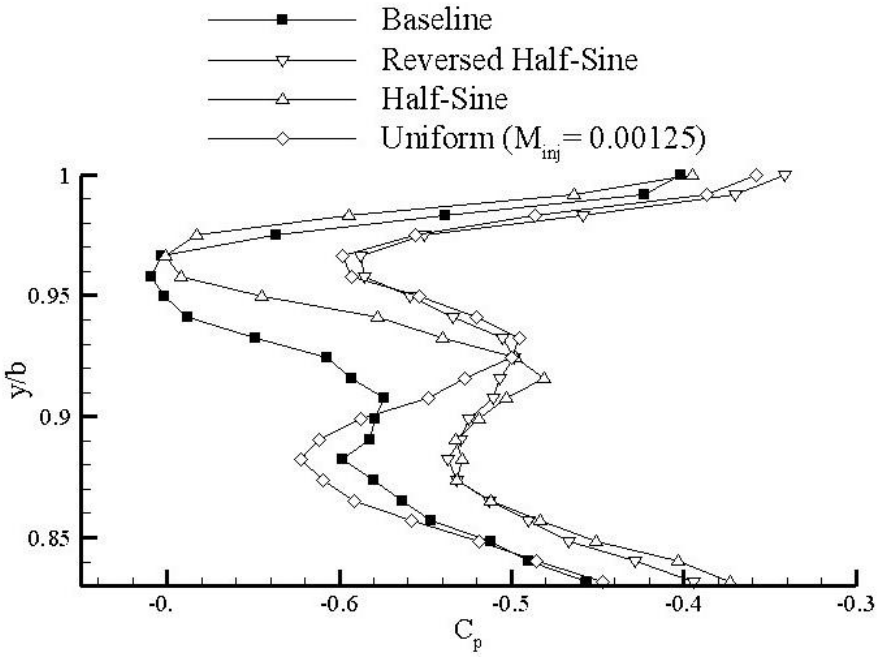

Figure 3.28 Pitch averaged total pressure loss coefficient variations for three different injection waveforms and comparison with the no-injection case. All have M_{inj} = 0.00125

Table 3.3 Passage averaged total pressure loss coefficients and pressure loss reduction levels for different waveforms and comparison with the no injection case. All have M_{inj}=0.00125

M_{inj}	Waveform Pattern	C_{μ}	$C_{p,passage}$	Pressure Loss Reduction (%)
0	Baseline	0	-0.578	0
0.00125	Reversed Half-Sine	0.078	-0.496	14.110
0.00125	Half-Sine	0.078	-0.529	8.474
0.00125	Uniform	0.061	-0.531	8.091

Figure 3.29 shows inplane velocity magnitude contours that are measured by Tr-PIV system. At 50% and 75% span, tip injection does not have an effect on wake structures. At 85% span, where passage vortices are dominant, reversed triangular waveform decreases the velocity defect within the wake, in contrast uniform waveform pattern increases the velocity defect levels. At 95% span location, all injection scenarios decrease the velocity deficits within the wake zone. It must be noted that uniform injection seems to be most efficient waveform pattern. In Figure 3.30, mean vorticity magnitudes are presented for sinusoidal injection set. At 50% span, tip injection has no effect in the wake zone as expected. At 75% span, half-sine and uniform injection scenarios decreases the wake size. Tip injection has minor effects at 85% span but it must be noted that uniform waveform increases the mean vorticity levels, especially near the trailing edge of the test blade. At the leakage vortex zone, at 95% span, tip injection moves the wake through the suction side of the test blade. It must be noted that uniform injection is the most effective waveform by means of decreasing vorticity. Tip injection also affects the wake of the neighboring blade, all injection waveforms have similar effect but all three decrease the vorticity levels.

Figure 3.31 shows the turbulent kinetic energy contours. At 50% span, tip injection does not affect the wake characteristics. Half-sine and uniform injection decreases the size of the wake at 75% while reversed half-sine does not have a major effect. At 85% span, tip injection does not seem to change the turbulent kinetic energy levels of the wake. At 95% span tip injection decreases the turbulence levels within the leakage wake zone and uniform waveform pattern is the most effective pattern compare to sinusoidal patters. Also it must be noted that uniform waveform slightly decreases the turbulence levels within the leakage zone of the neighboring blade.

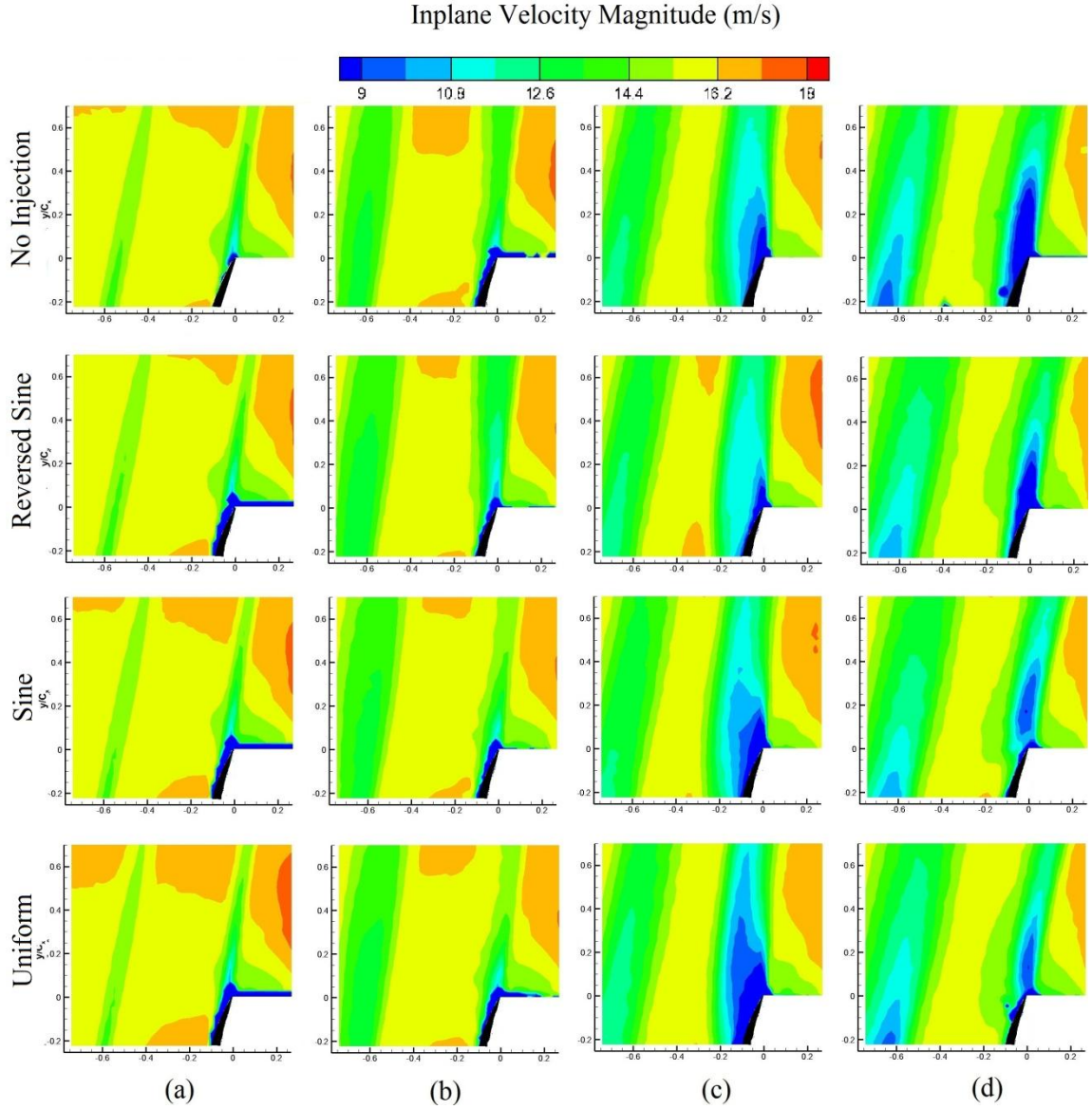

Figure 3.29 In-plane mean velocity magnitude contours for different injection waveform patterns where M_{inj}=0.00125 at (a) 50% (b) 75% (c) 85% and (d) 95% span. Lower right hand corner is blocked by shadow. The black zone is the trailing edge of the test blade. The flow is from bottom to top

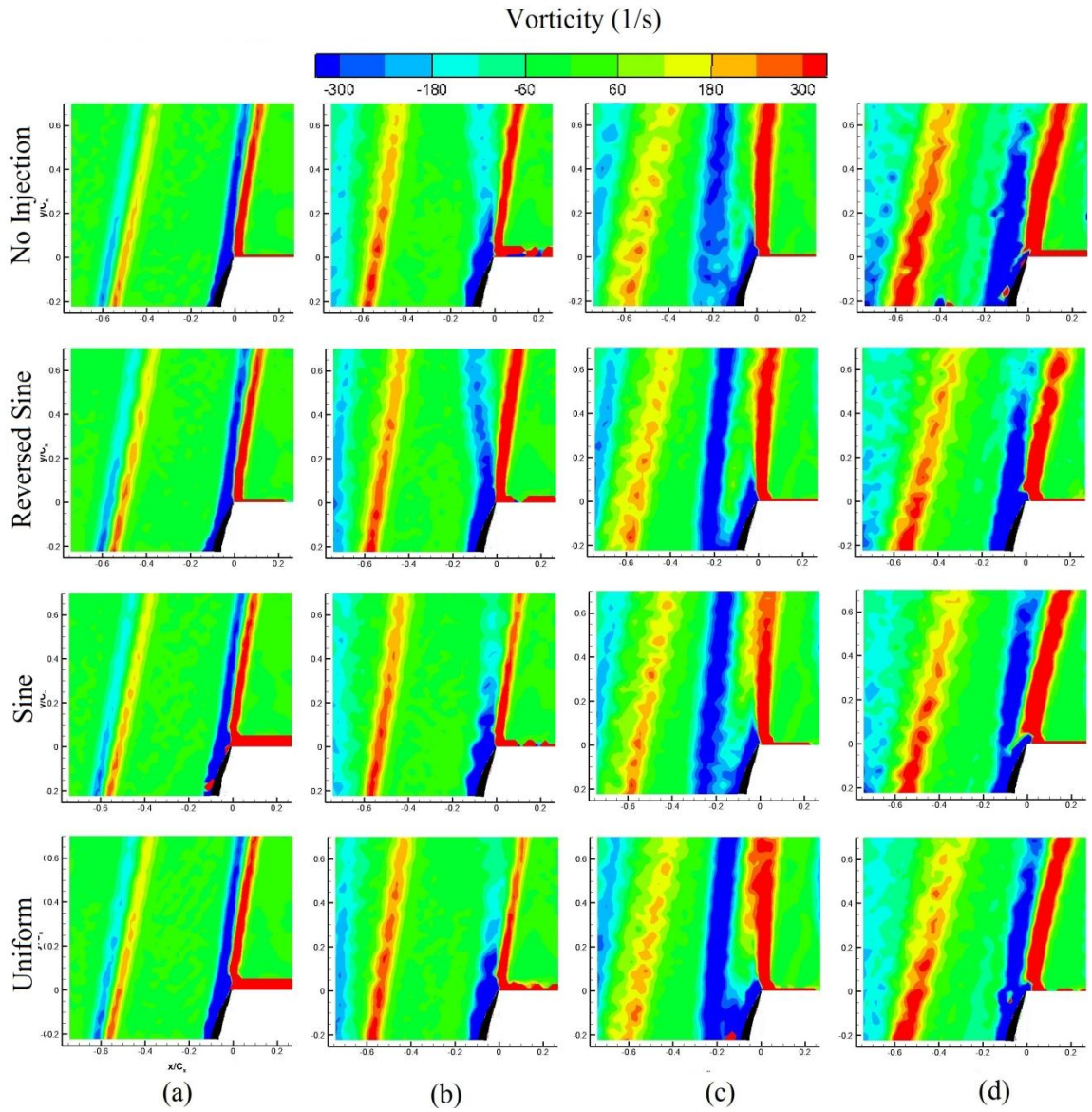

Figure 3.30 Mean vorticity (Ω_z) magnitude contours for different injection waveform patterns where M_{inj}=0.00125 at (a) 50% (b) 75% (c) 85% and (d) 95% span. Lower right hand corner is blocked by shadow. The black zone is the trailing edge of the test blade. The flow is from bottom to top

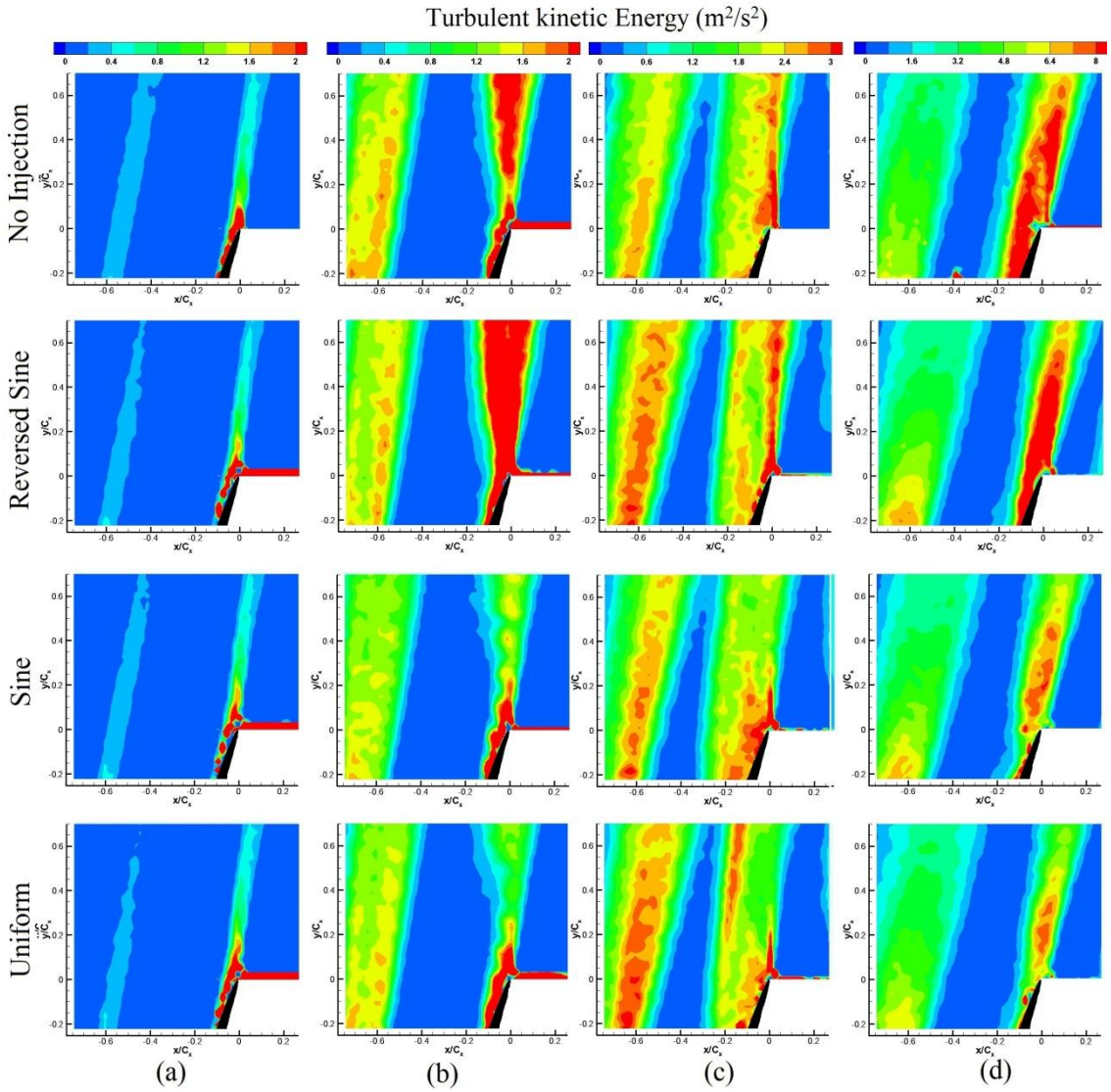

Figure 3.31 Turbulent kinetic energy contours for different injection waveform patterns where M_{inj}=0.00125 at (a) 50% (b) 75% (c) 85% and (d) 95% span. Lower right hand corner is blocked by shadow. The black zone is the trailing edge of the test blade. The flow is from bottom to top

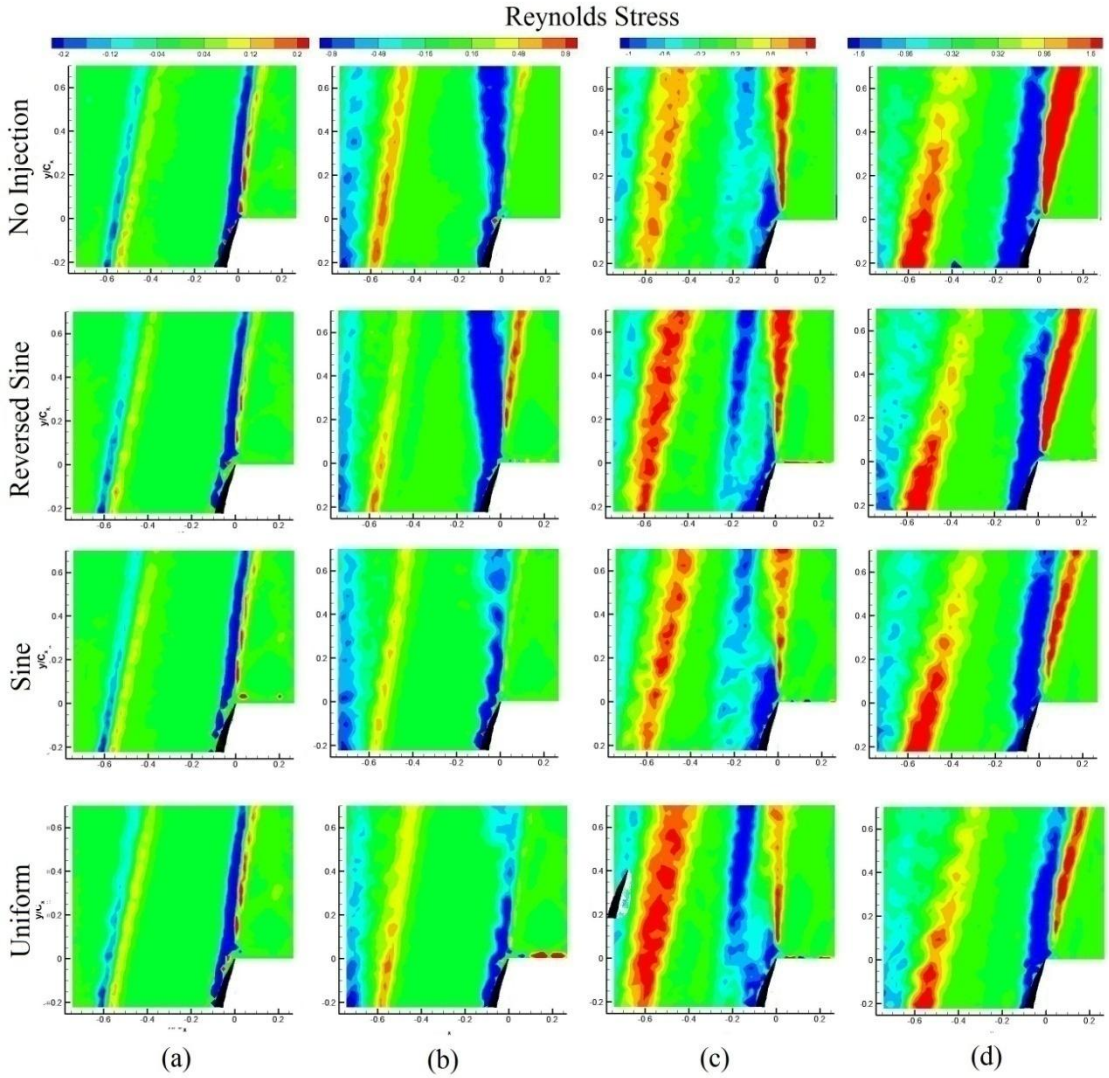

Figure 3.32 Reynolds shear stress contours for different injection waveform patterns where M_{inj}=0.00125 at (a) 50% (b) 75% (c) 85% and (d) 95% span. Lower right hand corner is blocked by shadow. The black zone is the trailing edge of the test blade. The flow is from bottom to top

Computed Reynolds shear stresses are presented in Figure 3.32. As expected, tip injection does not affect the wake characteristics at 50% span. At 75% span, uniform and half-sine waveform patterns decrease the stress levels within the wake, in contrast, reversed half-sine waveform increases the stress levels. At 85% span there is a slight increase at the stress levels when there is injection. In the leakage wake zone, i.e. at 95% span, all injection scenarios decrease the stress levels within the wake. It is clear that uniform injection is more effective than sinusoidal waveform by means of decreasing stress levels. Also tip injection decreases the stress levels within the leakage wake of the neighboring blade.

Figure 3.33 shows the wake center movements. At 50% span tip injection slightly moves the wakes away from the suction side. At 75% span, half-sine and uniform waveforms moves the wakes through the suction side, in contrast, reversed triangle pushes the wake inside the passage flow. At 85% span, it seems that tip vortex moves the wake away from the suction side, but this movement has been explained in section 3.4.1. in leakage vortex region, i.e. at 95% span, all injection scenarios move the wake near the suction side.

In Figure 3.34, wake center velocities are presented. At midspan, tip injection has minor effects on the wake characteristics. At 75% span, only reversed half-sine waveform has a major effect on the wake center velocity and decreases the center velocity which can be discussed as a negative effect. In passage vortex region, at 85% span, sinusoidal waveform patterns have minor effects on the center velocity but uniform waveform injection decreases the wake center velocity. At 95% span, tip injection increases the wake center velocity. Most effective pattern is reversed half-sine waveform which increases the wake center velocity up to %15 compared to no-injection case. Figure 3.35shows wake half-widths. At 50% span, there is no change when tip injection is present. At 75% span, reversed half-sine increases the wake half-width which means that size of the wake is increased. In other hands, uniform and half-sine waveform patterns decrease the wake size up to 35%. At 85% span, until 0.2 axial chord downstream, tip injection increases the size of the wake. After that point, size of the wake decreases. In the leakage vortex zone, at 95% span, all injection scenarios decrease the size of the wake. Sinusoidal waveforms have similar

effects. Uniform pattern, which is the most effective one, creates a size decrease up to %35 compared to no-injection case.

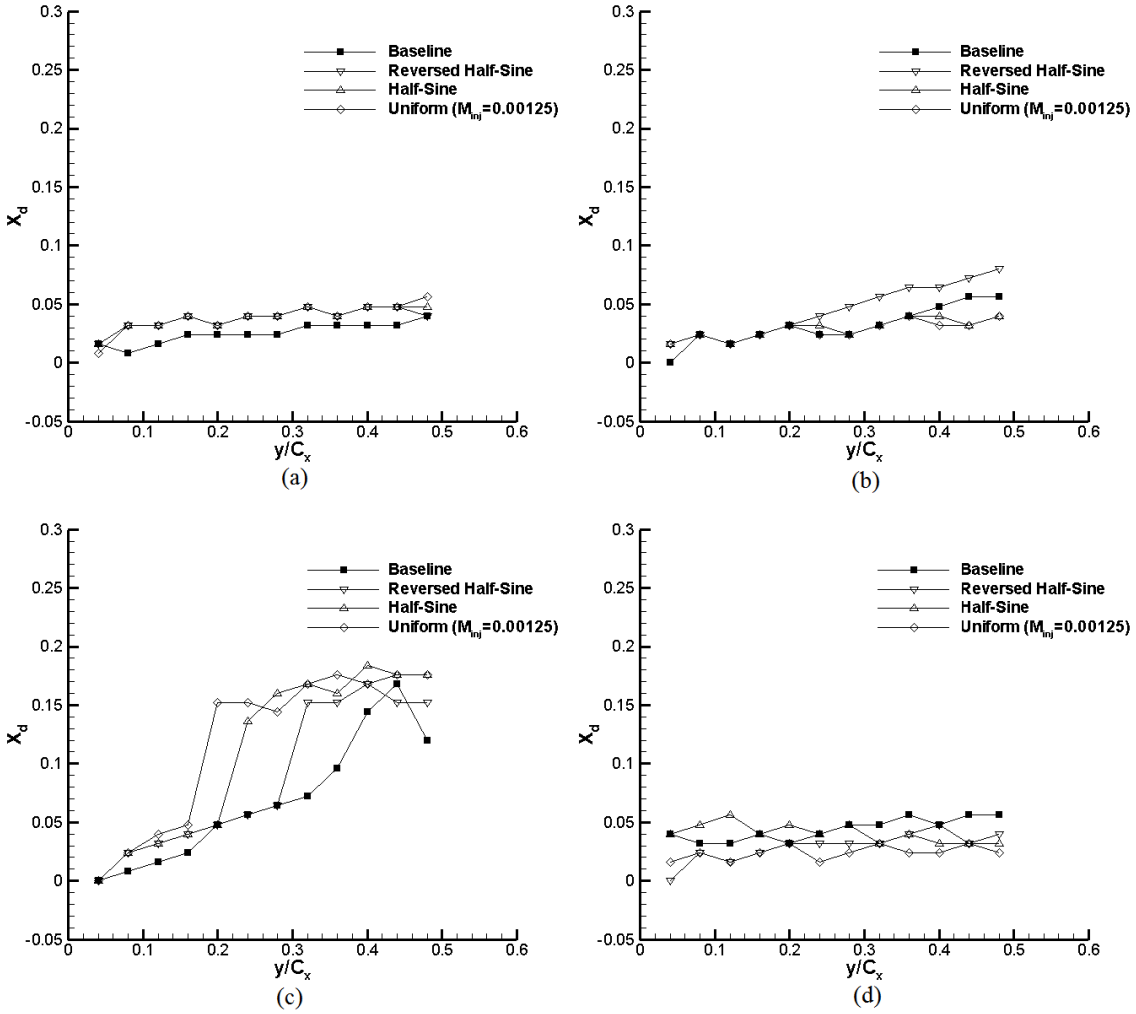

Figure 3.33 Wake center movementsthrough streamwise direction for different injection waveform patterns where M_{inj}=0.00125 at (a) 50% (b) 75% (c) 85% and (d) 95% span location

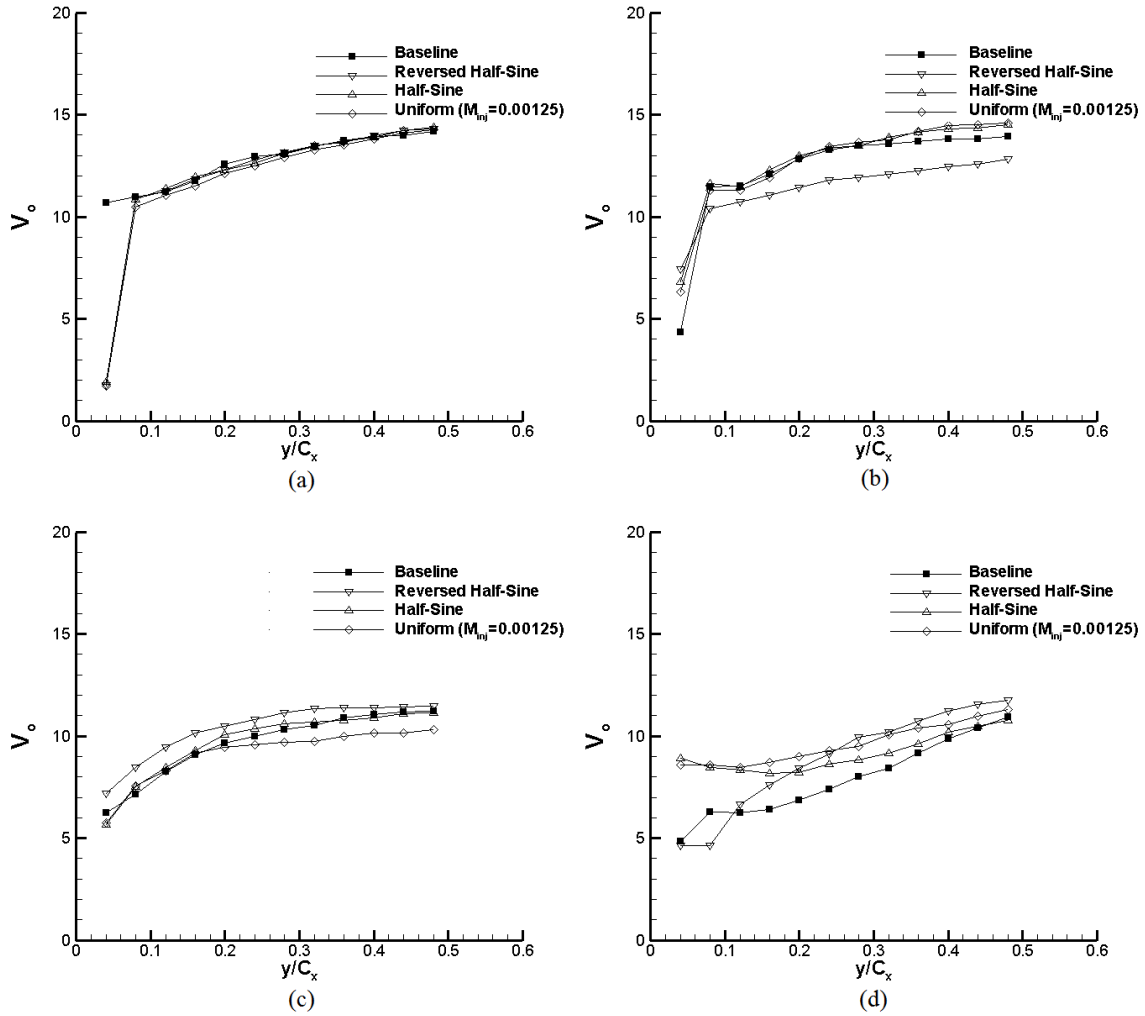

Figure 3.34 Wake center velocitiesthrough streamwise direction for different injection waveform patterns where M_{inj}=0.00125 at (a) 50% (b) 75% (c) 85% and (d) 95% span location

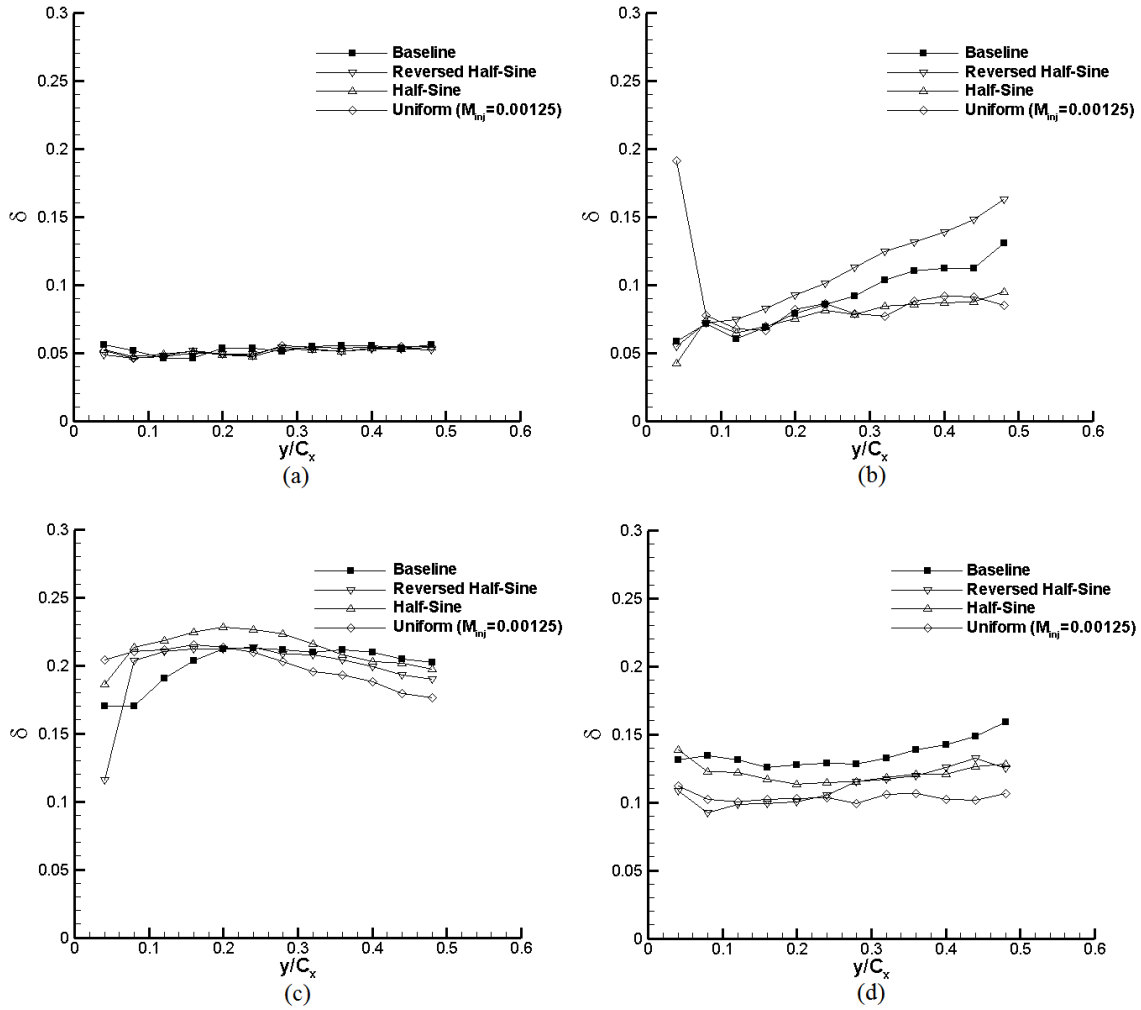

Figure 3.35 Wake half-widthsthrough streamwise direction for different injection waveform patterns where M_{inj}=0.00125 at (a) 50% (b) 75% (c) 85% and (d) 95% span location

CHAPTER 4

CONCLUSIONS AND DISCUSSIONS

In this thesis, the effect of camberwise modulated tip injection with different waveform patterns on tip leakage characteristics of a low pressure turbine cascade are investigated. The measurements are performed in a blow-down wind tunnel. The cascade blade row consists of five blades with all having T-106 blade profile. Total pressure measurements are conducted by traversing a Kiel probe 0.5 axial downstream of the blade rows.

The tip injection control mechanism consists of ten independent holes each connected to a solenoid valve. To understand the effects, two standpoints are determined. First one is to investigate the effects of injection mass flow rate ratio (the ratio of injected mass flow rate to total inlet mass flow rate) all having the same waveform pattern. Second one investigates the effect of injection waveform pattern for a constant injection mass flow rate ratio.

All tip injection scenarios have an effect on tip leakage vortex, also on passage vortex. The size of the vortex gets smaller, also vortex moves to the endwall. Injection mass flow rate ratio has an effect on the passage vortex of the test blade. As the ratio increases. Total pressure loss decreases. Secondary flow regions of the neighboring blade are also gets affected by the tip injection. As injection mass flow rate ratio increases, leakage vortex of the neighboring blade gets smaller and pressure loss within the vortex decreases. Passage vortex region of the neighboring blade does not seem to be affected by the control mechanism.

Triangular and half sine waveform patterns have similar effects on the characteristics of leakage vortex. Also reversed sine, reversed triangle and uniform waveforms are seem to be more effective on tip leakage vortex. The most reduction in ototal pressure loss is obtained in reversed waveform patterns. Reversed waveform patterns and uniform waveform patterns which having the same injection mass flow rate ratio seem to have a similar effect on leakage vortex region. But reversed waveform has more reduction in total pressure loss for the 10passage vortex region.

Future work in order to improve this study can focus on three different topics which are,

- To investigate the effects on the velocity domain, constant temperature hot-wire anemometry measurements can be conducted
- To examine the effects of injection angle, different test blade can be manufactured and same experimental procedure may be applied
- To compare the results detailed computational fluid dynamics solutions may be conducted.
- To understand the physics of the flow, experiments inside the gap without/with injection can be conducted

REFERENCES

[1] Yamamoto, A., 1988, “Interaction Mechanisms Between Tip Leakage Flow and the Passage Vortex in a Linear Turbine Rotor Cascade”, *ASME J. of Turbomachinery*, 110, 329-338

[2] Booth, T. C., 1985, “Importance of Tip Leakage Flow In Turbine Design”, *VKI Lecture Series*, 1985-05

[3] Gregory-Smith, D. G., Cleak, J. G. E., 1992, "Secondary Flow Measurement In a Turbine Cascade With High Inlet Turbulence", ASME J. of Turbomachinery, 114, 173-183

[4] Wiedner, B., 1994, " Passage Flow Structure and Its Influence on Endwall Heat Transfer In a Ninety Degree Turning Duct", Ph.D. Thesis, The Pennsylvania State University

[5] Bindon, J. P., 1989, “The Measurement and Formation of Tip Clearance Loss”, *ASME J. of Turbomechinery*, 111, 257-263, 88-GT-203

[6] Heyes, F. J. G., Hudson, H. P., 1993, “Measurement and Prediction of Tip Clearance Flow in Linear Turbine Cascades”, ASME J. of Turbomachinery, Vol. 115, 376-382

[7] Yaras, M., Zhu, Y., Sjolander, S. A., 1989, "Flow Field In the Tip Gap of a Planar Cascade of Turbine Blades", ASME J. of Turbomachinery, 111, 276-283

[8] Bindon, J. P., 1987, “The Measurementof Tip Clearance Flow Structure on the Endwall and Within the Clearance Gap of an Axial Turbine Cascade”, Proc. ImechE Int. Conference Turbomachinery-Efficiency Prediction and Improvement, Cambridge, United Kingdom, C273/87

[9] Sieverding, C. H., 1985, “Recent Progress in the Understanding of Basic Aspects of Secondary Flows in Turbine Blade Passages”, ASME J. of Turbomachinery, Vol 114, 248-257

[10] Gregory-Smith, D. G., 1997, “Physics of Secondary Flows”, VKI Lecture Series, 1997-01

[11] Langston, L. S., 2000, “Secondary Flow in Axial Turbines- A Review”, Presented atICHMT Turbine Symposium 2000, Cesme, Turkey

[12] Dey, D., Camci, C., “Aerodynamic Tip Desensitization of an Axial Turbine Rotor Using Tip Platform Extensions”, 2001, ASME Paper, 2001-GT-484

[13] Van Ness II, D. K., Corke, T. C., Morris, S. C., 2008, “Tip Clearance Flow Visualization of a Turbine Blade Cascade With Active and Passive Flow Control”, Proc. ASME Turbo Expo 2008, Berlin, Germany, GT2008-50703

[14] Rao, N. M., Camci, C., 2004, “Axial Turbine Tip Desensitization By Injection from a Tip Trench”, Proc. ASME Turbo Expo 2004, Vienna, Austria, GT2003-53256

[15] Ostovan, Y. 2011, “Experimental ınvestigation of Waveform Tip Injection on the Characteristics of the Tip Vortex”, M.Sc. Thesis, Middle East Technical University

[16] Uzol, O., Camci, C., 2005, “Heat Transfer, Pressure Loss and Flow Field Measurements Downstream of Staggered Two-Row Circular and Elliptical Pin Fin Arrays”, ASME Journal of Heat Transfer, Vol.127, No. 5, pp. 458-471

[17] Mercan, B., Ostovan, Y., Doğan, E., Uzol, O., 2010, “Effect of Chordwise Modulated Waveform Tip Injection on the Characteristics of the Tip Vortex” AIAA 40th Fluid Dynamics Conference and Exhibit, Chicago, Illinois, June 28-July 1 2010

[18] Von Ellenrieder, K. D., Pothos, S., 2007, “PIV Measurements of the Asymmetric Wake of a Two-Dimensional Heaving Airfoil,” Experiments in Fluids, Vol. 44, No. 5, pp. 733-745

[19] Uzol, O., Brzozowski, D., Chow, Y. –C., Katz, J., Meneveau, C., 2007, “A Database of PIV Measurements within a Turbomachinery Stage and Sample Comparisons with unsteady RANS,” Journal of Turbulence, Vol. 8

[20] Thomas, F. O., Liu, X., 2004, “An Experimental Investigation of Symmetric and Asymmetric Turbulent Wake Development in Pressure gradient”, Physics of Fluids, Vol. 16, Number 5, 1725-1745

[21] Chow, Y., Uzol, O., Katz, J., Meneveau, C., 2005, “Decomposition of the Spatially Filtered and Ensemble Averaged Kinetic Energy, the Associated Fluxes and Scaling Trends in a Rotor Wake”, Physics of Fluids, Vol. 17

[22] Mercan, B., Ostovan, Y., Uzol, O., 2011, "Experimental Investigation of the Effect of Uniform/Waveform Tip Injection in a Low Pressure Turbine Cascade", 11th International Conference on Fluid Control, Measurements and Visualization (FLUCOME), Keelung, Taiwan, Dec 5-9 2011

[23] Mercan, B., Doğan, E., Ostovan, Y., Uzol, O., 2011, "Experimental Investigation of the Effects of Waveform Tip Injection in a Low Pressure Turbine Cascade", ASME Turbo Expo 2012, Copenhagen, Denmark, June 11-15 2012